TR-170-2

OPTIMAL STOCHASTIC GUIDANCE LAWS FOR TACTICAL MISSILES

1 September 1971

Prepared for the

OFFICE OF NAVAL RESEARCH
AERONAUTICS PROGRAMS, CODE 461
DEPARTMENT OF THE NAVY
ARLINGTON, VIRGINIA 22217

Under

Contract Number N00014-69-C-0391

Prepared by:

Charles F. Price

Approved by:

Arthur A. Sutherland, Jr.
Arthur Gelb

THE ANALYTIC SCIENCES CORPORATION
6 Jacob Way
Reading, Massachusetts 01867

UNCLASSIFIED
Security Classification

DOCUMENT CONTROL DATA - R & D

(Security classification of title, body of abstract and indexing annotation must be entered when the overall report is classified)

1. ORIGINATING ACTIVITY (Corporate author)
The Analytic Sciences Corporation
6 Jacob Way
Reading, Massachusetts 01867

2a. REPORT SECURITY CLASSIFICATION
Unclassified

2b. GROUP

3. REPORT TITLE

Optimal Stochastic Guidance Laws for Tactical Missiles

4. DESCRIPTIVE NOTES (Type of report and inclusive dates)
Technical Report

5. AUTHOR(S) (First name, middle initial, last name)
Charles F. Price

6. REPORT DATE	7a. TOTAL NO. OF PAGES	7b. NO. OF REFS
1 April 1971	103	15

8a. CONTRACT OR GRANT NO.	9a. ORIGINATOR'S REPORT NUMBER(S)
N00014-69-C-0391	TR-170-2
b. PROJECT NO.	
c.	9b. OTHER REPORT NO(S) (Any other numbers that may be assigned this report)
d.	

10. DISTRIBUTION STATEMENT
Qualified requesters may obtain copies of this report from DDC.

11. SUPPLEMENTARY NOTES	12. SPONSORING MILITARY ACTIVITY
	Office of Naval Research Department of the Navy Arlington, Virginia 22217

13. ABSTRACT

Guidance laws are developed for tactical missiles which take into account the following important dynamic and random effects: random target motion, homing sensor measurement noise, bounded control level, bounded acceleration level, and missile autopilot dynamics. Several different guidance laws are derived using optimal stochastic control theory and evaluated by computer simulation. An important conclusion of this work is that when intercept accuracy is appreciably limited by missile maneuvering capability, a control policy obtained by taking control saturation into account can yield significantly better performance than control policies derived assuming that control levels are unconstrained.

DD FORM 1 NOV 68 1473 REPLACES DD FORM 1473, 1 JAN 64, WHICH IS OBSOLETE FOR ARMY USE.

UNCLASSIFIED
Security Classification

14. KEY WORDS	LINK A		LINK B		LINK C	
	ROLE	WT	ROLE	WT	ROLE	WT
Missile Guidance Optimal Guidance Homing Guidance Optimal Nonlinear Stochastic Control Laws Terminal Control						

FOREWORD

The author wishes to express appreciation for the encouragement and support provided by Mr. David Siegel of the Office of Naval Research. Acknowledgement is also made to Professor John J. Deyst, Jr. of the Massachusetts Institute of Technology for his helpful contributions relative to optimal nonlinear stochastic guidance laws.

ABSTRACT

Guidance laws are developed for tactical missiles which take into account the following important dynamic and random effects: random target motion, homing sensor measurement noise, bounded control level, bounded acceleration level, and missile autopilot dynamics. Several different guidance laws are derived using optimal stochastic control theory and evaluated by computer simulation. An important conclusion of this work is that when intercept accuracy is appreciably limited by missile maneuvering capability, a control policy obtained by taking control saturation into account can yield significantly better performance than control policies derived assuming that control levels are unconstrained.

TABLE OF CONTENTS

LIST OF FIGURES

LIST OF FIGURES (Continued)

1. INTRODUCTION

1.1 BACKGROUND AND OBJECTIVES

The task of guiding a tactical missile to a target is affected by a number of factors and constraints -- e.g., target maneuvering capability, homing sensor measurement errors, missile autopilot dynamics, bounded control variables, limited missile maneuvering capability, and launch initial conditions. To overcome those effects, a number of guidance techniques have been developed and evaluated (Refs. 1, 2, 3, 4, 5, 6). Heretofore, most guidance laws have been derived assuming fairly simple mathematical models of the missile-target engagement problem. A familiar example is so-called proportional guidance which is designed primarily for constant velocity targets and unconstrained missile controls. It is frequently found that guidance laws derived in this fashion yield terminal miss distances that are unacceptable when applied in situations where target maneuvers, etc., exist. Consequently one is motivated to obtain improved performance by including within the guidance problem formulation more of those factors which affect the missile's interception capability.

In Ref. 6 a number of guidance laws which offer improvements over conventional proportional guidance are evaluated. These laws are derived with the aid of optimal control theory from mathematical models that include the effects of initial condition errors, missile airframe dynamics, constant target acceleration and a penalty on the amount of control effort consumed. This report represents a continuation of that effort; guidance laws are developed which include the effects of measurement noise, bounded control levels, bounded maneuvering acceleration level and random time-varying target maneuvers. Emphasis is placed upon those

techniques which can potentially be applied in practical tactical missile weapons systems in the next ten to twenty years, especially those which can take advantage of the rapid improvement in computer hardware technology.

In Chapter 2 guidance laws are derived using some results from optimal stochastic control theory described in Appendix A, which account for measurement noise, random target acceleration, and bounded missile control variables. Performance results for these laws, obtained by computer simulation, are presented in Chapter 3. In addition, an acceleration limiting technique is developed and evaluated in Chapter 3, its purpose being to prevent the missile lateral acceleration from exceeding prescribed limits. A summary of the results and major conclusions are given in Chapter 4.

2. OPTIMAL STOCHASTIC GUIDANCE LAWS

In this chapter stochastic guidance problems for a tactical missile, including the effects of bounded control variables and sensor measurement errors, are formulated and solved. First a mathematical model is developed which provides a standard description of the guidance system dynamics for use throughout the report. Then both optimal and suboptimal nonlinear guidance laws are derived; the performance of each law is subsequently evaluated in Chapter 3 by digital computer simulations of the system model.

2.1 PROBLEM FORMULATION

The equations of motion for the missile guidance problem are derived assuming motion is confined to a single plane and neglecting forces caused by gravity and aerodynamic drag.* Referring to Fig. 2.1-1, a nonrotating orthogonal coordinate system is defined with the x-axis chosen along the line-of-sight (LOS) between the interceptor and the target at the beginning of the engagement. The center of the coordinate system moves with the target but the coordinate axes do not rotate.

*In actual applications, drag can significantly reduce the airspeed of a coasting missile, thereby adversely affecting guidance accuracy. The exclusion of this effect here is justified on the basis that we are seeking guidance law design criteria that offer improvement over conventional methods with respect to more significant guidance error sources. However, a more complete system evaluation of the methods resulting from this study would certainly include aerodynamic forces, as well as other factors neglected in this simplified investigation.

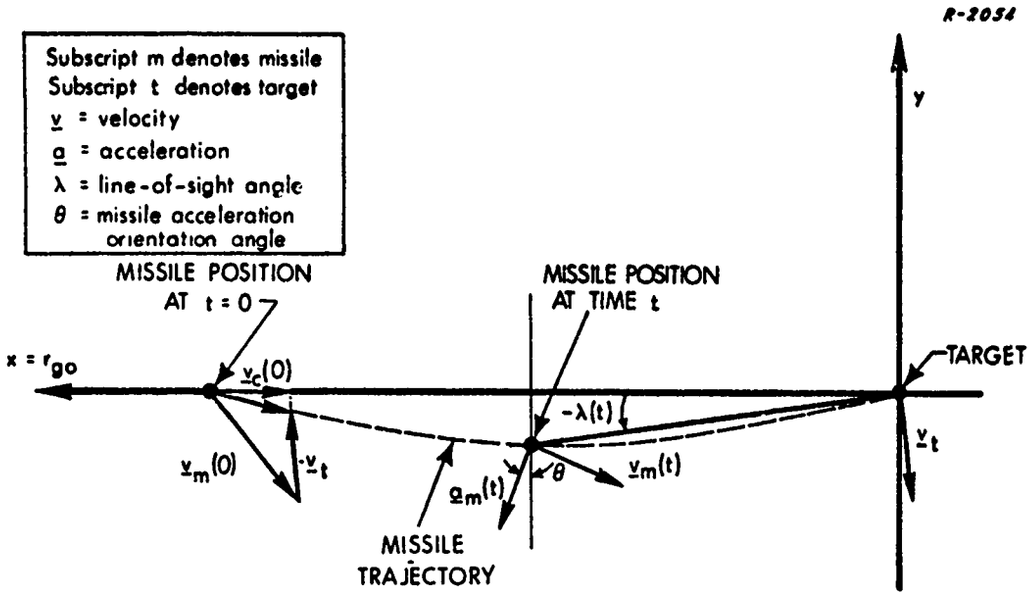

Figure 2.1-1 Relative Coordinate System

If the guidance system works well, a reasonable conjecture is that the LOS rotates very little along the missile's trajectory, except near the end when the range becomes small (less than 100 feet). This assumption is suggested by the similarity between optimal linear deterministic guidance laws and conventional proportional guidance in that all such techniques tend to achieve a small LOS angular rate (Refs. 5, 6). Consequently at the terminal time t_f, the missile trajectory intersects the y-axis in Fig. 2.1-1 almost perpendicularly and the terminal miss distance is approximately $y(t_f)$. Therefore, the missile's motion parallel to the y-axis is of primary interest.

We shall assume that the control variable available for the guidance law is the output u(t) of the missile's control actuation mechanism -- e.g., a control surface deflection.* The latter, acting through the missile

*This assumption neglects actuator dynamics which typically have much faster response characteristics than the missile rotational dynamics.

rotational dynamics, provides an acceleration vector $\underline{a}_m$ that changes the interceptor's flight path. In a nonthrusting drag-free vehicle, $\underline{a}_m$ is approximately perpendicular to the missile's velocity as indicated in Fig. 2.1-1. Only the y-component of $\underline{a}_m$, given by

$$a_{m_y} = -a_m(t) \cos \theta \qquad (2.1\text{-}1)$$

where $a_m(t) = |\underline{a}_m(t)|$, is important for controlling terminal miss. If the orientation of $\underline{v}_m$ is assumed to be slowly varying, $\cos \theta$ can be treated as a known scale factor; throughout this discussion we assume $\cos \theta = 1$.

In many applications the missile rotational equations of motion can be modeled as being linear; therefore they can be written in state variable form as

$$\begin{aligned} \dot{\underline{x}}_m(t) &= F_m \underline{x}_m(t) + \underline{g}_m u(t) \\ a_m(t) &= \underline{c}_m^T \underline{x}_m(t) + du(t) \end{aligned} \qquad (2.1\text{-}2)$$

where the acceleration is regarded as an output variable that in general can be a function of both the state $\underline{x}_m(t)$ and the control $u(t)$.* In this report F_m, $\underline{g}_m$, $\underline{c}_m$, and d are assumed to be constant arrays, a condition that needs some elaboration. In many applications missile dynamic characteristics vary rapidly because of changing flight conditions, especially when thrusting at a high g-level. In these situations, the parameters in Eq. (2.1-2) may be treated as constant if an adaptive autopilot has been designed which maintains known, uniform dynamic characteristics.

*For example, in a tail-controlled lifting vehicle u(t) can represent the control surface deflection which contributes directly to missile lateral acceleration.

Alternatively, when the elements of F_m, etc., are time-varying, they can be estimated on-line by a parameter identification technique which can track time-varying parameters. In either case, the subsequent development has application; however we shall see that if the airframe parameters are known a priori, certain feedback control gains can be determined off-line and stored in the guidance computer. If the parameters are identified in flight, then the control gains must be calculated on-line.

In addition to the missile's acceleration, the target acceleration $\underline{a}_t(t)$ has an effect on the guidance dynamics. In particular, from Fig. 2.1-1 it follows that

$$\ddot{y}(t) = a_{t_y}(t) + a_{m_y}(t) \qquad (2.1\text{-}3)$$

where $a_{t_y}(t)$ is the component of $\underline{a}_t$ along the y-axis. We shall assume that the target accelerates randomly according to the relations

$$\dot{\underline{x}}_t = F_t \underline{x}_t(t) + \underline{w}_t(t)$$

$$a_{t_y}(t) = \underline{c}_t^T \underline{x}_t(t) \qquad (2.1\text{-}4)$$

where $\underline{w}_t(t)$ is a gaussian white noise process having statistics described by*

$$E\left\{\underline{w}_t(t)\right\} = \underline{0}$$

$$E\left\{\underline{w}_t(t)\,\underline{w}_t(\tau)^T\right\} = Q_t \delta(t-\tau) \qquad (2.1\text{-}5)$$

*A nonzero, known mean can readily be included in the development.

and F_t and $\underline{c}_t$ are known constant arrays. The matrix Q_t is constant and positive semidefinite, and $\delta(t-\tau)$ is the unit impulse function. This model represents the target's acceleration as the output of a linear system driven by white noise. It is a good representation insofar as the target maneuvers appear to be random and correlated in time. The correlation characteristics of $a_{t_y}(t)$, which determine the extent to which the target's future maneuvers can be predicted from previous measurements of target motion, are determined by F_t.

Random maneuvers are frequently used by aircraft flying in a region where they are subject to attack by missiles, especially by surface-to-air missiles (SAM's) (Ref. 7). The pilot's purpose is to prevent SAM radar trackers from acquiring a fix on the aircraft. However, if the pilot knows a SAM has been launched, he is more likely to employ one of several deterministic-type maneuvers which have been historically successful in avoiding intercepts. To analyze the latter situation, game theory may allow a more realistic problem formulation in that the target aircraft can be modeled as an intelligent evader whose objective is to maximize the terminal miss distance. In this report only random target motion is considered; the application of game theory is an important topic for future investigation.

Combining Eqs. (2.1-2), (2.1-3), and (2.1-4) the complete set of state equations for the guidance problem can be written as*

*The symbols $\underline{0}$ and $[0]$ denote respectively a vector and a matrix having all elements zero.

$$\frac{d}{dt}\begin{bmatrix} y(t) \\ \dot{y}(t) \\ \underline{x}_t(t) \\ \underline{x}_m(t) \end{bmatrix} = \begin{bmatrix} 0 & 1 & \underline{0}^T & \underline{0}^T \\ 0 & 0 & \underline{c}_t^T & -\underline{c}_m^T \\ \underline{0} & \underline{0} & F_t & [0] \\ \underline{0} & \underline{0} & [0] & F_m \end{bmatrix}\begin{bmatrix} y(t) \\ \dot{y}(t) \\ \underline{x}_t(t) \\ \underline{x}_m(t) \end{bmatrix} + \begin{bmatrix} 0 \\ -d \\ \underline{0} \\ \underline{g}_m \end{bmatrix} u(t) + \begin{bmatrix} 0 \\ 0 \\ \underline{w}_t(t) \\ \underline{0} \end{bmatrix} \quad (2.1\text{-}6)$$

or more compactly as

$$\dot{\underline{x}}(t) = F\underline{x}(t) + \underline{g}u(t) + \underline{w}(t) \quad (2.1\text{-}7)$$

where*

$$\underline{x}(t) \triangleq \begin{bmatrix} y(t) \\ \dot{y}(t) \\ \underline{x}_t(t) \\ \underline{x}_m(t) \end{bmatrix}; \qquad \underline{w}(t) \triangleq \begin{bmatrix} 0 \\ 0 \\ \underline{w}_t(t) \\ \underline{0} \end{bmatrix}$$

$$E\left\{\underline{w}(t)\,\underline{w}(\tau)^T\right\} \triangleq Q\,\delta(t-\tau) = \begin{bmatrix} 0 & 0 & \underline{0}^T & \underline{0}^T \\ 0 & 0 & \underline{0}^T & \underline{0}^T \\ \underline{0} & \underline{0} & Q_t & [0] \\ \underline{0} & \underline{0} & [0] & [0] \end{bmatrix} \delta(t-\tau) \quad (2.1\text{-}8)$$

and F and $\underline{g}$ are identified as the matrix and vector coefficients of $\underline{x}(t)$ and u(t) respectively, in Eq. (2.1-6). The initial value of $\underline{x}(t)$ is assumed to be a vector gaussian random variable with known statistics given by

*The notation $\underline{0}$ and [0] denotes respectively a vector and a matrix having all zero elements.

$$E\{\underline{x}(0)\} = \underline{\mu}$$

$$E\left\{[\underline{x}(0) - \underline{\mu}][\underline{x}(0) - \underline{\mu}]^T\right\} = P_0$$

The objective in designing the guidance system is to derive a feedback control law for u(t) having performance that is optimum in some sense. In order to provide feedback, measurements related to the elements of $\underline{x}(t)$ must be available. It is usually realistic to assume that measurements of line-of-sight angle or angle rate are available from a homing sensor. From Fig. 2.1-1, the LOS angle $\lambda(t)$ is given approximately by

$$\lambda(t) \cong \frac{y(t)}{x(t)} = \frac{y(t)}{v_c(t_f - t)} \qquad (2.1\text{-}9)$$

where t_f is the terminal time and v_c is the magnitude of the closing velocity which is assumed to be constant. If Eq. (2.1-9) is differentiated with respect to time, the result is

$$\dot{\lambda}(t) \cong \frac{1}{v_c}\left[\frac{y(t)}{(t_f - t)^2} + \frac{\dot{y}(t)}{(t_f - t)}\right] \qquad (2.1\text{-}10)$$

Consequently, within the limits of the approximation stated in Eq. (2.1-9), an LOS rate measurement is linearly related to the state variables y(t) and $\dot{y}(t)$. In addition, linear measurements of some of the missile airframe state variables $\underline{x}_m(t)$ (pitch rate, lateral acceleration, etc.) are also generally available. The set of all these measurements, $\underline{z}(t)$, is considered to be available at discrete times t_i and corrupted by additive gaussian noise; thus $\underline{z}(t_i)$ can be expressed as

$$\underline{z}(t_i) \triangleq \underline{z}_i = H_i\underline{x}_i + \underline{v}_i \qquad (2.1\text{-}11)$$

where

$$H_i = \begin{bmatrix} 1/v_c(t_f - t_i)^2 & 1/v_c(t_f - t_i) & \underline{0}^T & \underline{0}^T \\ \underline{0} & \underline{0} & [0] & H_m \end{bmatrix}$$

$$E\{\underline{v}_i\} = \underline{0}$$

$$E\left\{\underline{v}_i \underline{v}_j^T\right\} = \begin{cases} R_i & ; \quad i = j \\ 0 & ; \quad i \neq j \end{cases} \qquad (2.1\text{-}12)$$

and R_i is a positive definite matrix that can vary with time. The quantity $\underline{x}_i$ denotes $\underline{x}(t_i)$ in Eq. (2.1-7) and the matrix H_m describes the linear relation between the missile airframe state variables and the measurements.

In situations where the homing sensor output is interpreted as an LOS angle, H_i takes the form

$$H_i = \begin{bmatrix} 1/v_c(t_f - t_i) & 0 & \underline{0}^T & \underline{0}^T \\ \underline{0} & \underline{0} & [0] & H_m \end{bmatrix}$$

In this report we use Eq. (2.1-12) as the sensor model.

In order to guide the missile, the measurement data is to be used for computing control commands. To allow for the time required to make the necessary calculations, it is assumed that a new value of the control can be computed only at each measurement time t_i. Thus on the interval $t_i \leq t \leq t_{i+1}$, $u(t)$ is held constant at the value of $u(t_i)$. Because both the measurements and the controls are generated at discrete points in time, we use the discrete equivalent of Eq. (2.1-7):

$$u_i \triangleq u(t_i) ; \qquad \underline{x}_i \triangleq \underline{x}(t_i)$$

$$\underline{x}_{i+1} = \Phi_i \underline{x}_i + \underline{\gamma}_i u_i + \underline{w}_i \qquad (2.1\text{-}13)$$

where Φ_i, $\underline{\gamma}_i$, and $\underline{w}_i$ are determined from F, $\underline{g}$, and $\underline{w}(t)$ according to Eqs. (A.1-12) and (A.1-13) of Appendix A. For this application the interval between measurements is assumed to be of uniform length, Δt,

$$\Delta t \triangleq t_{i+1} - t_i; \qquad i = 0, 1, \ldots, N-1$$

with $t_N \triangleq t_f$. Therefore, because the dynamics in Eq. (2.1-7) and the statistics of $\underline{w}(t)$ are constant, Eqs. (2.1-13), (A.1-12) and (A.1-13) can be written as

$$\begin{aligned} \Phi_i &= \Phi \triangleq e^{F\Delta t} \\ \underline{\gamma}_i &= \underline{\gamma} \triangleq \int_0^{\Delta t} e^{F(\Delta t - \tau)}\, \underline{g}\, d\tau \\ \underline{x}_{i+1} &= \Phi \underline{x}_i + \underline{\gamma} u_i + \underline{w}_i; \qquad i = 0, 1, \ldots, N-1 \end{aligned} \tag{2.1-14}$$

where $\underline{w}_i$ is a gaussian random sequence satisfying

$$\begin{aligned} E\{\underline{w}_i\} &= \underline{0} \\ E\{\underline{w}_i \underline{w}_i^T\} \triangleq Q_d &= \int_0^{\Delta t} e^{F(\Delta t - \tau)}\, Q \left(e^{F(\Delta t - \tau)}\right)^T d\tau \\ E\{\underline{w}_i \underline{w}_j^T\} &= 0; \qquad i \neq j \end{aligned} \tag{2.1-15}$$

Having Eqs. (2.1-11) and (2.1-14) describing the measurement sequence and the discrete time dynamics, we desire to establish rational performance criteria for determining each control u_i. In many applications the most important objective is that the terminal miss distance be made as

small as possible. More precisely, if we define a loss function of the terminal miss distance $f(x_1(t_f))$, where x_1 is the first element of the state vector $\underline{x}$ -- i.e., the quantity y in Fig. 2.1-1 -- and t_f is the terminal time, then we say that guidance performance is optimized if the index

$$J = E\left\{f(x_1(t_f))\right\}$$

is minimized. The designer's objective is to determine the sequence of optimal control commands which accomplishes this goal. In this report the loss function used is the square of the miss distance so that the performance index becomes

$$J_1 = E\left\{x_1(t_f)^2\right\} \qquad (2.1\text{-}16)$$

In practical applications the allowable values of the control are bounded in magnitude; typically for tactical missiles the control surface deflection is limited to a few degrees. Thus, our objective is to minimize J_1 subject to the constraint*

$$|u_i| \leq D\,; \qquad i = 0,1,\ldots,N\text{-}1 \qquad (2.1\text{-}17)$$

It is subsequently demonstrated that this problem formulation leads to an optimal nonlinear stochastic control law; i.e., u_i is a nonlinear function of past measurements.

*Depending upon the type of control actuation mechanism in use, it may be desirable to restrict other variables as well, say du/dt. Such a requirement can complicate the task of finding the optimal control law and the designer may have to settle for a suboptimal law that satisfies the constraints but which does not exactly minimize J_1.

If the energy expended by the control law is of no importance, as may be the case in short range missions or near the end of a long range mission, the above problem formulation is quite realistic. Its solution will indicate the ultimate guidance accuracy that can be achieved for a given target engagement situation when control level is bounded. However, for comparison purposes it is convenient to consider alternative performance criteria that have been advocated for the guidance problem.

In (Ref. 6) linear guidance laws for a continuous-time, deterministic problem formulation are evaluated. These laws are chosen to minimize a quadratic performance index of the form

$$J = x_1(t_f)^2 + r\int_0^{t_f} u(t)^2\,dt \qquad (2.1\text{-}18)$$

for various models of the missile autopilot dynamics and target maneuvering capability, but without any direct constraint on $|u(t)|$. This performance criterion has one advantage over that outlined above, in that the presence of u(t) in the definition of J results in a guidance law that tends to conserve missile energy.* However, it lacks a capability for directly

*This statement must be qualified with respect to the type of energy consumption one is talking about. If the control surface actuator is electromagnetic, a constant electric current must be provided to maintain a constant control surface deflection and $\int u(t)^2\,dt$ is proportional to the electrical energy consumed. However, in electrohydraulic systems, power is required only when the control surface is in motion so that $\int \dot{u}(t)^2\,dt$ is a better measure of energy. In addition, some systems pump hydraulic fluid into the atmosphere; in this case $\int |\dot{u}(t)|\,dt$ represents the amount of fluid expended. Besides actuator energy/fluid losses, the missile incurs a kinetic energy loss proportional to $\int |a(t)|\,dt$ when it performs a maneuver at constant altitude. Although J in Eq. (2.1-18) is directly related only to energy used by the electromagnetic type of actuator, it is frequently observed that utilizing a penalty on the integral of $u(t)^2$ produces a control law that also tends to limit all of the other losses mentioned above. Therefore we are qualitatively correct in saying that minimization of J in Eq. (2.1-18) tends to conserve missile energy.

constraining control magnitude. Therefore the control levels called for can exceed any limit which may exist; this condition tends to occur most frequently near the expected time of intercept when the observed line-of-sight angular rate tends to become large.

By analogy with Eq. (2.1-18), in this study we investigate a performance index having a quadratic penalty on control level, to be compared with J_1 in Eq. (2.1-16). Namely, we seek those unconstrained controls u_i which minimize the index

$$J_2 = E\left\{x_1(t_f)^2 + r \sum_{i=0}^{N-1} u_i^2\right\} \qquad (2.1\text{-}19)$$

This design criterion ordinarily leads to a linear stochastic control law; i.e., u_i is a linear function of the measurements. However, because the actual missile control capability is constrained according to Eq. (2.1-17), the control sequence obtained by minimizing J_2 is "clipped" when applied in the actual guidance system resulting in a suboptimal nonlinear stochastic guidance law.

The solutions to the above two guidance problems are given in the next two sections.

2.2 OPTIMAL NONLINEAR STOCHASTIC GUIDANCE LAW

The optimal stochastic guidance problem associated with Eqs. (2.1-16) and (2.1-17) is summarized as follows:

Given the linear discrete time dynamic relations

$$\underline{x}_{i+1} = \Phi \underline{x}_i + \gamma u_i + \underline{w}_i \qquad (2.2\text{-}1)$$

with linear measurements

$$\underline{z}_i = H_i \underline{x}_i + \underline{v}_i \qquad (2.2\text{-}2)$$

determine the optimal sequence of controls* u_i^o ($i = 0, 1, \ldots, N-1$) such that the performance index

$$J_1 = E\left\{x_1(t_f)^2\right\} \tag{2.2-3}$$

is minimized, subject to the constraint

$$|u_i| \leq D ; \qquad \text{for all } i \tag{2.2-4}$$

Definitions of the quantities Φ, $\underline{\gamma}$, H_i, $\underline{w}_i$, and $\underline{v}_i$ are available in Eqs. (2.1-12), (2.1-14) and (2.1-15). The above problem formulation is a discrete-time generalization of the case treated by Nahi and Sworder (Ref. 8); the latter is a continuous time problem which does not take into account target or autopilot dynamics. Fortunately the optimal guidance law is readily obtained as described in Appendix A. Its mechanization can be described as two separate functions.

First, a conventional Kalman filter is implemented to obtain an estimate $\hat{\underline{x}}_i$ of the state $\underline{x}_i$. The required filtering equations, taken from Eqs. (A.2-1) and (A.2-4), are as follows:

$$\begin{aligned}
\tilde{P}_0 &= P_0 ; \qquad \tilde{\underline{x}}_0 = \underline{\mu} \\
K_i &= \tilde{P}_i H_i^T \left(H_i \tilde{P}_i H_i^T + R_i\right)^{-1} \\
\hat{\underline{x}}_i &= \tilde{\underline{x}}_i + K_i\left(\underline{z}_i - H_i \tilde{\underline{x}}_i\right) \\
P_i &= \tilde{P}_i - K_i\left(H_i \tilde{P}_i H_i^T + R_i\right) K_i^T \\
\tilde{P}_{i+1} &= \Phi P_j \Phi^T + Q_d \\
\tilde{\underline{x}}_{i+1} &= \Phi \hat{\underline{x}}_i + \underline{\gamma} u_i^o ; \qquad i = 0, 1, \ldots N-1
\end{aligned} \tag{2.2-5}$$

*The superscript "o" denotes optimal.

where $\underline{\mu}$ and P_0 are the initial mean and covariance matrix of the state, and $\underline{\tilde{x}}_i$ and $\tilde{P}_i$ denote respectively the estimate and its corresponding covariance matrix just before a measurement is taken.

To obtain the second part of the solution -- i.e., the method for calculating u_i^o-- we begin by transforming $\underline{\hat{x}}_i$ linearly according to Eq. (A.4-8) to obtain the quantity $\underline{\hat{y}}_i$; the latter is the expected value of the terminal state, given $E\{\underline{x}(t_i)\} = \underline{x}_i$, if no control is applied during the interval $t_i \le t \le t_N$. Because Φ is independent of time, $\underline{\hat{y}}_i$ becomes

$$\underline{\hat{y}}_i = \Phi^{N-i}\,\underline{\hat{x}}_i \tag{2.2-6}$$

where we have made the substitution

$$\Phi(t_N, t_i) = \Phi^{N-i}$$

Actually only the first element, $\hat{y}_{1_i}$, of the transformed state is needed. If the first row of Φ^{N-i} is defined to be a transposed column vector, $\underline{\varphi}_i^T$, we have

$$\hat{y}_{1_i} = \underline{\varphi}_i^T\,\underline{\hat{x}}_i \tag{2.2-7}$$

Similarly, the vector $\underline{\gamma}$ in Eq. (2.2-1) is transformed according to Eq. (A.4-6) to obtain the quantity $\underline{\delta}_i$, which represents the effect on the terminal state of a constant control $u(t) = u_i$ applied during the interval $t_i \le t \le t_{i+1}$;

$$\underline{\delta}_i = \Phi^{N-i-1}\,\underline{\gamma} \tag{2.2-8}$$

Only the first element of $\underline{\delta}_i$ is needed to describe the effect of the control on the terminal miss distance; therefore by analogy with Eq. (2.2-7) we calculate

$$\delta_{1_i} = \underline{\varphi}_{i+1}^T\,\underline{\gamma} \tag{2.2-9}$$

where $\underline{\varphi}_{i+1}$ is the first row of Φ^{N-i-1}. Now the optimal control strategy, as proved in Appendix A, is to select a control such that the total predicted terminal miss produced by both $\hat{\underline{x}}_i$ and u_i be as close to zero as possible; i.e., we desire

$$\hat{y}_{1_i} + \delta_{1_i} u_i = 0$$

remembering that the constraint in Eq. (2.2-4) must also be satisfied. Consequently the optimal nonlinear control law (see Eq. (A.4-17)) is given by

$$u_i^o = \begin{cases} -\hat{y}_{1_i}/\delta_{1_i} & ; \quad \left|y_{1_i}/\delta_{1_i}\right| \le D \\ -D \operatorname{sgn}\left(\hat{y}_{1_i}/\delta_{1_i}\right); & \left|y_{1_i}/\delta_{1_i}\right| > D \end{cases}$$

or alternatively

$$\boxed{\begin{aligned} u_i^o &= \begin{cases} -\underline{d}_i^T \underline{x}_i & ; \quad \left|\underline{d}_i^T \underline{x}_i\right| \le D \\ -D \operatorname{sgn}\left(\underline{d}_i^T \underline{x}_i\right); & \left|\underline{d}_i^T \underline{x}_i\right| > D \end{cases} \\ \underline{d}_i &\triangleq \frac{1}{\delta_{1_i}} \underline{\varphi}_i ; \qquad i = 0, 1, \cdots, N-1 \end{aligned}} \qquad (2.2\text{-}10)$$

Thus the complete guidance law is represented as a linear filter cascaded with a nonlinear control policy; the latter consists of a set of gains $\underline{d}_i$ followed by an amplitude limiter. A block diagram of the system is given in Fig. 2.2-1. We shall refer to the entire sequence of the optimal control as $\{u_i^o\}$.

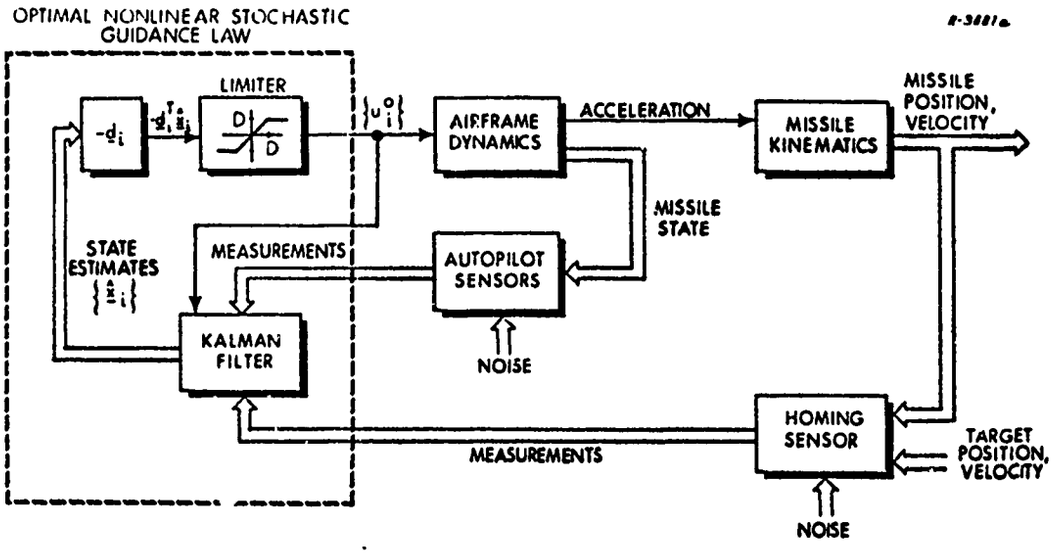

Figure 2.2-1 Optimal Nonlinear Stochastic Guidance Law

At this point it is worth mentioning that the guidance law derived above is much more general than implied by the statement of the guidance problem at the beginning of this section. It is proved in Section A.4 that the control sequence given in Eq. (2.2-10) minimizes any convex symmetric function of the terminal miss distance subject to the constraint in Eq. (2.2-4). Consequently one can say that, in a very broad sense, this guidance law yields the best possible terminal accuracy, within the missile's control capability.

The mechanization of Eqs. (2.2-5) and (2.2-10) requires computation of both the set of Kalman filter gains K_i and the feedback gains $\underline{d}_i$, given by

$$\underline{d}_i = \frac{1}{\underline{\varphi}_{i+1}^T \underline{\gamma}} \underline{\varphi}_i$$

First, with respect to the feedback gains, both $\underline{\varphi}_i$ and $\underline{\varphi}_{i+1}$ are derived from the matrices Φ^{N-i} and Φ^{N-i-1}. The latter usually can be determined

analytically in this application. We have already noted that Φ^{N-i} is the transition matrix $\Phi(t_f, t_i)$ associated with Eq. (2.1-7). Because F is time-invariant, it follows that

$$\Phi\left(t_f, t_i\right) = \Phi\left(t_f - t_i, 0\right) \tag{2.2-11}$$

An analytical expression for $\Phi(t, 0)$ as a function of t can be obtained by applying Laplace transforms to the homogeneous equation

$$\dot{\underline{x}}(t) = F\,\underline{x}(t)$$

associated with Eq. (2.1-7). The result is

$$\Phi(t, 0) = L^{-1}\left[(Is - F)^{-1}\right] \tag{2.2-12}$$

where

$$(Is - F)^{-1} = \begin{bmatrix} \frac{1}{s} & \frac{1}{s^2} & \frac{1}{s^2}\underline{c}_t^T(Is - F_t)^{-1} & -\frac{1}{s^2}\underline{c}_m^T(Is - F_m)^{-1} \\ 0 & \frac{1}{s} & \frac{1}{s}\underline{c}_t^T(Is - F_t)^{-1} & -\frac{1}{s}\underline{c}_m^T(Is - F_m)^{-1} \\ 0 & 0 & (Is - F_t)^{-1} & [0] \\ 0 & 0 & [0] & (Is - F_m)^{-1} \end{bmatrix} \tag{2.2-13}$$

and $L^{-1}[\ ]$ denotes the inverse Laplace transform. The vectors $\underline{\varphi}_i$ and $\underline{\varphi}_{i+1}$ are determined by evaluating the first row of Eqs. (2.2-12) and (2.2-13) and by substituting respectively the quantities $(t_f - t_i)$ and $(t_f - t_{i+1})$ for t into Eq. (2.2-12). Carrying out the inversion operation indicated in Eq. (2.2-12) is straightforward and leads to fairly simple expressions for the elements of $\underline{\varphi}_i$ and $\underline{\varphi}_{i+1}$ when the dimensions of F_t and F_m are not too large.

The elements of $\underline{\varphi}_i$ and $\underline{\varphi}_{i+1}$ vary with the index i, requiring knowledge of time-to-go which is given by

$$t_{go} = \frac{\text{range-to-go}}{v_c}$$

assuming that the closing velocity, v_c, is constant. In practice, v_c is not exactly constant so that t_{go} must be continually estimated from measurements of range and range rate. Consequently, in the form presented here, the optimal stochastic guidance law is applicable only for those missiles having a radar homing sensor, or some other method of measuring range. If various simplifications are made -- such as modeling the noise as being independent of range, using constant filter gains, neglecting autopilot dynamics, etc., the requirement for range measurements can be eliminated; however it is expected that system performance will be somewhat degraded.

The Kalman filter gains K_i in Eq. (2.2-5) are calculated from a time-varying nonlinear difference equation. Generally it is most practical to compute these gains on-line because H_i depends upon both the closing velocity (see Eq. (2.1-12)) and time-to-go, which are not known before the mission.

2.3 SUBOPTIMAL NONLINEAR STOCHASTIC GUIDANCE LAW

The optimal stochastic guidance problem associated with Eq. (2.1-19) is summarized as follows:

Given the linear discrete-time dynamic relations

$$\underline{x}_{i+1} = \Phi \underline{x}_i + \underline{\gamma} u_i + \underline{w}_i \tag{2.3-1}$$

with linear measurements

$$\underline{z}_i = H_i \underline{x}_i + \underline{v}_i \tag{2.3-2}$$

determine the optimal sequence of controls $\{u_i^o\}$ $(i = 0, 1, \ldots, N-1)$ which minimizes the performance index

$$J_2 = E\left\{x_1(t_N)^2 + r \sum_{i=0}^{N-1} u_i^2\right\} \tag{2.3-3}$$

where r is a weighting constant selected by the designer. Definitions of the quantities Φ, $\underline{\gamma}$, H_i, $\underline{w}_i$, and $\underline{v}_i$ are available in Eqs. (2.1-12), (2.1-14) and (2.1-15).

The solution to the above problem can be taken directly from Section A.2; however, first it is convenient to modify Eq. (2.3-1) using the transformation technique described in Section A.4. Specifically, we define

$$\begin{aligned} \underline{y}_i &\triangleq \Phi^{N-i} \underline{x}_i \\ y_{1_i} &\triangleq \underline{\varphi}_i^T \underline{x}_i \end{aligned} \tag{2.3-4}$$

where $\underline{y}_i$ is the terminal state produced by an initial state $\underline{x}_i$ with no control or random forcing function applied, y_{1_i} is the first element of the vector $\underline{y}_i$, and $\underline{\varphi}_i^T$ is the first row of the matrix Φ^{N-i}. Substitution from Eq. (2.3-1) for $\underline{x}_{i+1}$ and $\underline{x}_i$ produces

$$\underline{y}_{i+1} = \underline{y}_i + \underline{\delta}_i u_i + \underline{\omega}_i \qquad (2.3\text{-}5)$$

where $\underline{\delta}_i$ and $\underline{\omega}_i$ are specified by Eqs. (A.4-6) and (A.4-7). Now the first element of the vector $\underline{y}_i$ is the terminal miss distance produced by the state at time t_i. Hence, using Eq. (2.3-4) we have

$$y_{1_N} = x_1(t_N) \qquad (2.3\text{-}7)$$

Therefore by substitution from Eqs. (2.3-4) through (2.3-7) into Eqs. (2.3-1) through (2.3-3), the linear optimal stochastic guidance problem can be restated as follows:

Given the linear discrete-time dynamic relations

$$\underline{x}_{i+1} = \Phi \underline{x}_i + \underline{\gamma} u_i + \underline{w}_i$$

$$y_{1_{i+1}} = y_{1_i} + \delta_{1_i} u_i + \omega_{1_i}$$

$$y_{1_i} = \underline{\varphi}_i^T \underline{x}_i \qquad (2.3\text{-}8)$$

with linear measurements

$$\underline{z}_i = H_i \underline{x}_i + \underline{v}_i \qquad (2.3\text{-}9)$$

determine the optimal sequence of controls $\{u_i^o\}$ $(i = 0, 1, \ldots, N-1)$ which minimizes the performance index

$$J_2 = E\left\{y_{1_N}^2 + r\sum_{i=0}^{N-1} u_i^2\right\} \qquad (2.3\text{-}10)$$

Although the above problem statement is apparently more complex than Eqs. (2.3-1) through (2.3-3), it permits the solution for the optimal controls to be more readily obtained. The latter follows directly from Section A.2. First a conventional Kalman filter is implemented to obtain an estimate $\hat{y}_{1_i}$ of y_{1_i}. This is done by first estimating $\underline{x}_i$ using Eq. (2.2-5) and then applying the transformation

$$\hat{y}_{1_i} = \underline{\varphi}_i^T \hat{\underline{x}}_i \qquad (2.3\text{-}11)$$

This part of the solution is almost identical to that for the nonlinear problem discussed in the preceding section; the only exception is that u_i^o is now computed differently, as indicated below.

We can derive $\{u_i^o\}$ with the aid of the scalar equation for $y_{1_{i+1}}$ (Eq. (2.3-8)) and the performance index in Eq. (2.3-10). Comparing these relations with Eqs. (A.2-1), (A.2-2), and (A.2-3) and making the identifications

$$\left.\begin{aligned} V_N &= 1 \\ V_i &= 0 \ ; \qquad i \neq N \\ W_i &= r \\ \underline{x}_i \text{ (in Eq. (A.2-2))} &= y_{1_i} \\ \Phi_i &= 1 \\ \Gamma_i &= \delta_{1_i} \end{aligned}\right\} \quad \text{for all } i \qquad (2.3\text{-}12)$$

we obtain the optimal control law

$$u_i^o = -c_i \hat{y}_{1_i} \tag{2.3-13}$$

where the scalar feedback gain c_i is computed from the backward recursion relations

$$c_i = s_{i+1} \delta_{1_i} \left(s_{i+1} \delta_{1_i}^2 + r \right)^{-1}$$

$$s_i = s_{i+1} - c_i^2 \left(s_{i+1} \delta_{1_i}^2 + r \right)$$

$$s_N = 1 \tag{2.3-14}$$

The control law in Eq. (2.3-13) is similar to "predictive proportional guidance" (Ref. 5) in the sense that u_i^o depends upon the predicted terminal miss distance, $\hat{y}_{1_i}$. The solution given here is somewhat more general because missile autopilot dynamics and target dynamics are included in the problem formulation.

To provide an analogy with the results obtained in the preceding section, we combine Eqs. (2.3-11) and (2.3-13) to obtain

$$u_i^o = -\underline{c}_i^T \hat{\underline{x}}_i$$

$$\underline{c}_i \triangleq c_i \underline{\varphi}_i \tag{2.3-15}$$

The gains $\underline{c}_i$ are distinguished from the gains $\underline{d}_i$ in Eq. (2.2-10) by the comparison between the scalar quantities $(1/\delta_{1_i})$ and c_i. The latter is the more difficult quantity to evaluate because no closed form solution is available for Eq. (2.3-14), whereas δ_{1_i} is obtained analytically. Because the

boundary condition on s_i is specified at the terminal time t_N, Eq. (2.3-14) is solved backward in time, and the feedback gain must be stored in the guidance computer.* This computational distinction is probably not important in applications where the dynamics of the guidance problem are known a priori, because the gains for each guidance law can be calculated off-line and approximated in storage as polynomial functions of time-to-go. However, if some important dynamic parameters -- such as those associated with the missile airframe -- are unknown and must be identified on-line, then the system gains must be calculated on-line. In the latter situation, the computational advantage of the optimal nonlinear law is more significant.

Thus far, the guidance law derived above can be represented as a linear filter cascaded with a linear control policy. In mechanizing the guidance equations, the control is first computed according to Eq. (2.3-4). If $|u_i^o| \leq D$, the linear control is applied; however, if $|u_i^o| > D$, the control level is "clipped" at the level $D\,\mathrm{sgn}\,(u_i^o)$ by the saturation inherent in the control actuator. Consequently, the actual applied control will in general be nonlinear; it is also suboptimal with respect to the objective of minimizing J_2. In order to distinguish the applied control surface deflection from that given in Eq. (2.2-10), we designate the entire sequence of controls generated by the procedure described above as $\{u_{i_o}\}$,

$$u_{i_o} = \begin{cases} -\underline{c}_i^T \hat{\underline{x}}_i \quad ; & |\underline{c}_i^T \hat{\underline{x}}_i| \leq D \\ -D\,\mathrm{sgn}\left(\underline{c}_i^T \hat{\underline{x}}_i\right); & |\underline{c}_i^T \hat{\underline{x}}_i| > D \end{cases} \tag{2.3-16}$$

*Perhaps an analytical solution can be obtained for the discrete-time feedback gain by making an analogy with the continuous-time case treated in Ref. 5. No attempt has been made here to resolve this question.

where the subscript "o" denotes that it is a suboptimal nonlinear guidance law. The adjective "suboptimal" applies in two contexts -- because of the nonlinearity in Eq.(2.3-16) $\{u_{i_o}\}$ does not generally achieve as low a value of J_2 as the unconstrained control; it also does not generally achieve as low a value of J_1 in Eq. (2.2-3) as the control law given in Eq. (2.2-10).

A block diagram of the above guidance law is given in Fig.2.3-1. It is observed by comparison with Fig. 2.2-1 that the functional structure of the suboptimal law is exactly the same as the optimal nonlinear law derived in the previous section. The difference in specific detail between the two is, as we have already noted, the manner in which the gains operating upon $\hat{\underline{x}}_i$ are computed. An evaluation of the intercept accuracy obtained using the controls defined in Eqs. (2.2-10) and (2.3-16) is given in the next chapter.

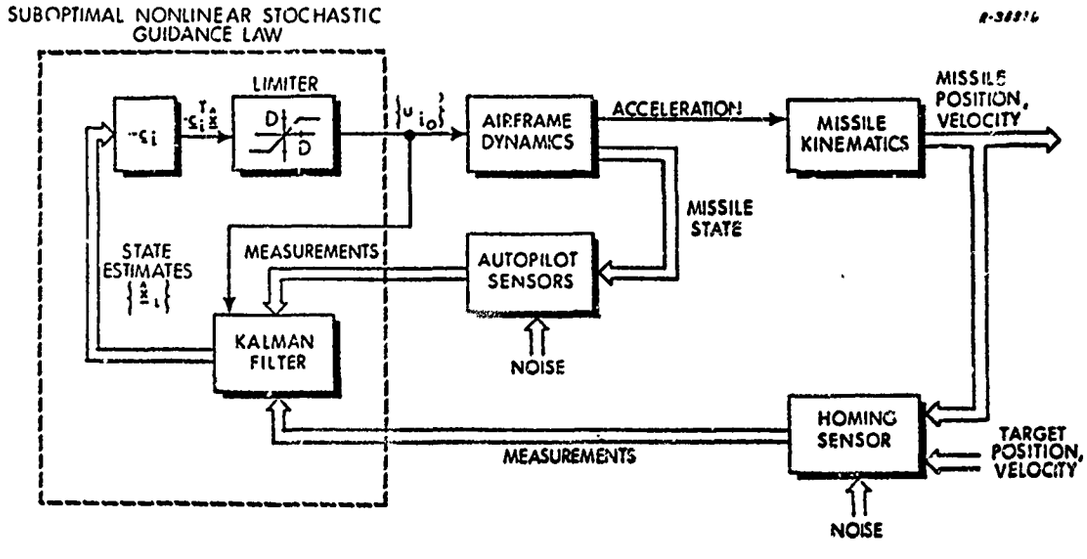

Figure 2.3-1 Suboptimal Nonlinear Stochastic Guidance Law

3. EVALUATION OF GUIDANCE LAWS

In this chapter the results of digital computer simulations of the optimal and suboptimal nonlinear guidance laws derived in Chapter 2 are presented. In addition, a method of limiting missile airframe lateral acceleration is proposed and evaluated. Statistical averages (root-mean-square values) of important quantities -- terminal miss distance, peak acceleration, etc. -- are computed from the results of twenty-five Monte Carlo runs performed for each of several different launch times and different values of the guidance problem parameters (measurement noise level, target acceleration level, etc.). These averages are determined empirically, rather than analytically, because the equations describing their evolution along the missile's trajectory are too complex* to solve for the number of different cases which we wish to examine.

3.1 CHOICE OF MATHEMATICAL MODELS

Missile Dynamics -- For this investigation the missile airframe dynamics are those of a vehicle that utilizes aerodynamic lift for its maneuvering force and has tail-mounted control surfaces and fixed wings. The missile is assumed to be in coasting (nonthrusting) flight with its equations of motion in the form of Eq. (2.1-2). For this type of missile, the airframe dynamic parameters are specified by

*This is a consequence of the fact that the guidance laws are nonlinear.

$$F_m = \begin{bmatrix} M_q & \dfrac{M_\alpha}{L_\alpha V} \\ VL_\alpha & -L_\alpha \end{bmatrix} \qquad g_m = \begin{bmatrix} M_\delta \\ -VL_\alpha L_\delta \end{bmatrix}$$

$$\underline{c}_m^T = [\,0 \quad 1\,] \qquad d = VL_\delta \qquad (3.1\text{-}1)$$

and the airframe state variables are

$$\underline{x}_m(t) \triangleq \begin{bmatrix} q(t) \\ a(t)' \end{bmatrix} \qquad (3.1\text{-}2)$$

The input u(t) is the control surface deflection angle. The symbols used in the above expressions are defined as follows:

$M_\alpha, M_q, M_\delta, L_\alpha, L_\delta$ = Stability derivatives

V = Airspeed

$q(t)$ = Pitch rate

$a(t)'$ = Normal acceleration produced by body-wing lift

We assume that all of the above parameters are constant and known and that q(t) and a(t)′ can be measured from rate gyro and accelerometer* outputs. This second order model describes the dominant planar rotational motion of the airframe.

*If an accelerometer is oriented along the lift vector and mounted at the missile center of gravity, its output, a(t), is related to a(t)′ by the relation (neglecting measurement noise):

$$a(t)' = a(t) - VL_\delta\, u(t)$$

Target Dynamics — The target motion has the random structure specified by Eq. (2.1-4). In this simulation the target acceleration a_{t_y} is assumed to be a first-order Markov process specified by the scalar quantities

$$F_t = f_t \qquad C_t = 1$$

$$Q_t = q_t = 2f_t\sigma^2 \tag{3.1-3}$$

That is, a_{t_y} satisfies the differential equation

$$\dot{a}_{t_y} = f_t\, a_{t_y} + w_t(t)$$

$$E\left\{w_t(t)\, w_t(\tau)\right\} = 2f_t\sigma^2\, \delta(t-\tau)$$

The covariance q_t of the white noise process which drives the target dynamics is expressed in terms of σ, the steady state root-mean-square (rms) target acceleration; i.e.,

$$\lim_{t\to\infty} E\left\{a_{t_y}(t)^2\right\} = \sigma^2$$

Measurement Noise — The measurements available for implementing the guidance laws are described by Eqs. (2.1-11) and (2.1-12). In this investigation it is assumed that the missile autopilot sensors directly observe both state variables, i.e.,

$$H_m = I \tag{3.1-4}$$

at uniform intervals of length Δt. The most important element of the measurement noise covariance matrix is r_{11}, the mean square value of the homing sensor noise. In a practical application, homing sensor noise

is contributed by the sensor receiver unit, the target itself (scintillation noise), the target environment, and the servo control loop used to direct the sensor. Some noise components decrease as range decreases (e.g., radar receiver noise); others increase as range decreases (e.g., target scintillation noise); others are range independent (e.g., sensor servo noise). For the purpose of providing a comparative evaluation of the guidance laws derived in Chapter 2, we choose r_{11} to be constant along a given trajectory with a value that is inversely proportional to the square of the launch range, r_ℓ. This simulates, in part, the effect of target scintillation noise, which is the most troublesome error source. The validity of this noise model improves as the launch range decreases. The expression from which r_{11} is calculated is

$$r_{11} = \left[\frac{2\sigma_s}{r_\ell(\Delta t)} \right]^2 \qquad (3.1\text{-}5)$$

The quantity, $\sigma_s/r_\ell(\Delta t)$, represents the standard deviation of the scintillation measurement error in line-of-sight rate at the instant of launch. This error is caused by the fact that radar reflections are returned from different points on the target from sample to sample because of the target's rotation relative to the missile and/or because of changes in radar transmitter frequency. The rms values of the separation between reflecting points is denoted by σ_s. The factor of two is inserted into Eq. (3.1-5) simply to allow for the fact that scintillation noise strength increases as the range to the target decreases. Thus r_{11} represents an "average" scintillation noise along the missile trajectory. This model provides a realistic sensor noise level, neglecting time-variation in the noise statistics.

Some qualification is needed for the assumption that the homing sensor noise samples in Eq. (2.1-11) are independent. This is not

realistic if the homing sensor is a radar that operates at constant frequency because then the scintillation effect is due solely to changes in the relative rotational orientation of the missile and target, which usually occur more slowly than the pulse repetition rate. However, it is often found desirable to use "frequency diversity" -- i.e., to change the transmitter frequency from pulse to pulse -- to frustrate jamming countermeasures taken by the target. In this case, successive scintillation noise samples tend to be independent. The latter situation has the more adverse effect upon guidance accuracy. If the error in line-of-sight angle has significant correlation over some number of adjacent pulses, the resulting error in measuring LOS rate is less than if the measurement errors are uncorrelated. Therefore, the model used here represents the worst type of scintillation noise.

Other sources of measurement noise are the autopilot sensors whose mean square levels are denoted by r_{22} (gyro noise) and r_{33} (accelerometer noise). These two parameters are also assumed to be constant. All three measurement errors are assumed to be uncorrelated with each other so that the off-diagonal terms in R_i are zero. Therefore R_i is a constant matrix, R, of the form

$$R_i = R = \begin{bmatrix} r_{11} & 0 & 0 \\ 0 & r_{22} & 0 \\ 0 & 0 & r_{33} \end{bmatrix}; \qquad i = 0,1,\ldots,N-1 \qquad (3.1\text{-}6)$$

3.2 SIMULATION RESULTS

In this section, both the optimal and suboptimal nonlinear control sequences derived in Chapter 2, $\{u_i^0\}$ and $\{u_{i_0}\}$ respectively, are evaluated from computer simulation results. The values of the parameters defined in Section 3.1 are given below:

Missile Airframe Parameters

$M_q = -0.455$ $\qquad$ $L_\alpha = 10.15$

$M_\alpha = -8.4$ $\qquad$ $L_\delta = 1.86$

$M_\delta = -71.2$ $\qquad$ $V = 2920$ ft/sec

Target Parameters

$$f_t = -0.3 \text{ sec}^{-1}$$

$$\sigma^2 = 9.0 \times 10^3 \left(\text{ft/sec}^2\right)^2$$

Measurement Parameters

$\Delta t = 0.05$ sec $\qquad$ $v_c = 2000$ ft/sec

$\sigma_s = 4.75$ ft $\qquad$ $r_{22} = 5.0 \times 10^{-6} (\text{rad/sec})^2$

$r_{33} = 10.0 \left(\text{ft/sec}^2\right)^2$

Initial State Statistics

$$\underline{\mu} = \underline{0}$$

$$P_0 = \begin{bmatrix} 0 & 0 & 0 & 0 & 0 \\ 0 & 0 & 0 & 0 & 0 \\ 0 & 0 & 9.0\times10^{3}(\text{ft/sec}^2)^2 & 0 & 0 \\ 0 & 0 & 0 & 1.0\times10^{-4}(\text{rad/sec})^2 & 0 \\ 0 & 0 & 0 & 0 & 1.0\times10^{3}(\text{ft/sec}^2)^2 \end{bmatrix}$$

The missile airframe parameter values given above are taken from Ref. 6, Appendix H. The target dynamics are chosen to yield a target acceleration correlation time constant of about three seconds. The two upper-left diagonal elements of the initial state covariance matrix, P_0, are taken to be zero, simulating the absence of an initial heading error. This is done so that the effects of target acceleration alone on terminal miss distance can be analyzed. Of course, appreciable heading errors can exist at launch -- especially at close ranges -- and their presence should be included in a complete quantitative evaluation of these guidance laws.

Another parameter to be selected is the weighting constant r that is associated with J_2 in Eq. (2.3-3) and which is needed to compute the suboptimal control sequence $\{u_{i_o}\}$, specified in Eq. (2.3-16). The value chosen for r should be such that the comparison between $\{u_i^o\}$ and $\{u_{i_o}\}$ is a fair one. For example, if r is large, the suboptimal law heavily penalizes the control level. This tends to yield small feedback gains, $\underline{c}_i$, in Eq. (2.3-16) and correspondingly small values of $|u_{i_o}|$, at the expense of a relatively large terminal miss distance. Thus, if terminal miss distance

is used as the basis of comparison, the optimal guidance law will be definitely superior; if the guidance laws are evaluated on the basis of control level, then the suboptimal law will appear to be superior. To avoid this ambiguity, we regard the level of terminal miss distance as the primary indicator of system performance; after all, miss distance is the sole quantity appearing in the performance index for the optimal nonlinear guidance law (Eq. (2.2-3)). We shall also be interested in the control levels required by both guidance laws, but this consideration will be of secondary importance. With these priorities in mind, r is chosen small enough so that any further reduction in its value produces no significant further reduction in the expected terminal miss distance; the value selected was ten.

The simulation consisted of substituting $\{u_i^o\}$ and $\{u_{i_o}\}$ from Eqs. (2.2-10) and (2.3-16) for $\{u_i\}$ in Eq. (2.2-1), beginning at a variety of launch ranges. Twenty-five Monte Carlo computer runs were made from each launch point; the random sequences $\{\underline{w}_i\}$ and $\{\underline{v}_i\}$ in Eqs. (2.2-1) and (2.2-2) were generated by a Gaussian random number generator. Because we are interested in the relative performance of $\{u_i^o\}$ and $\{u_{i_o}\}$, identical sets of random numbers are used in the simulation of each guidance law.

Figure 3.2-1 shows the performance of both guidance laws with the maximum control surface deflection, D in Eq. (2.2-4), set equal to 0.2 radian. In Fig. 3.2-1(a) the rms values of the terminal miss distance obtained using the optimal and suboptimal guidance laws are plotted for launch times ranging from one to six seconds before intercept. Note that the optimal law gives an accuracy only slightly superior to that of the suboptimal law.

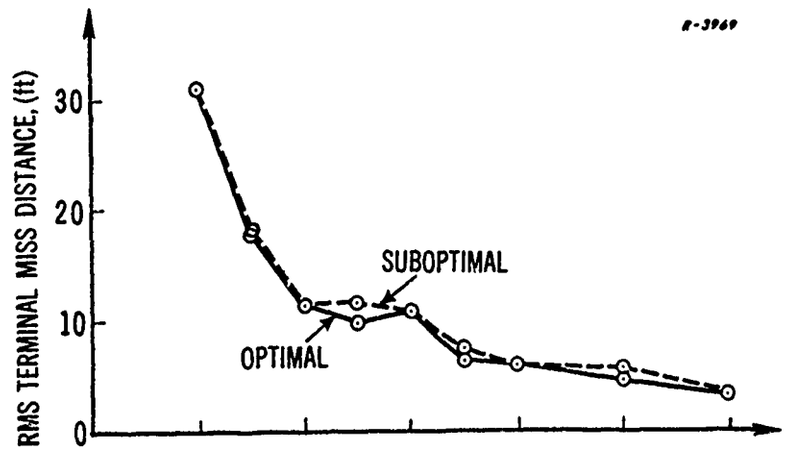

(a) Miss distance

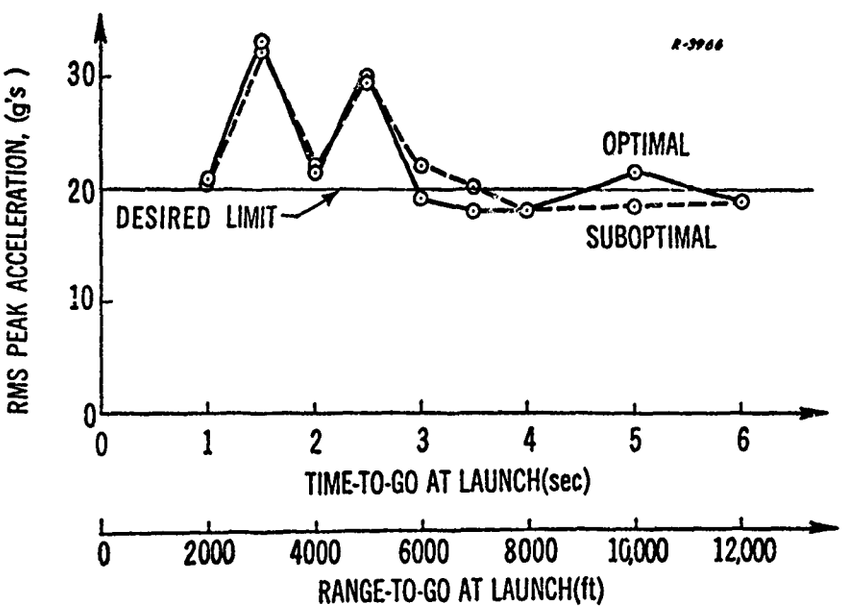

(b) Acceleration

Figure 3.2-1 **Guidance Law Performance Averaged Over Twenty-Five Monte Carlo Runs: D = 0.2 rad**

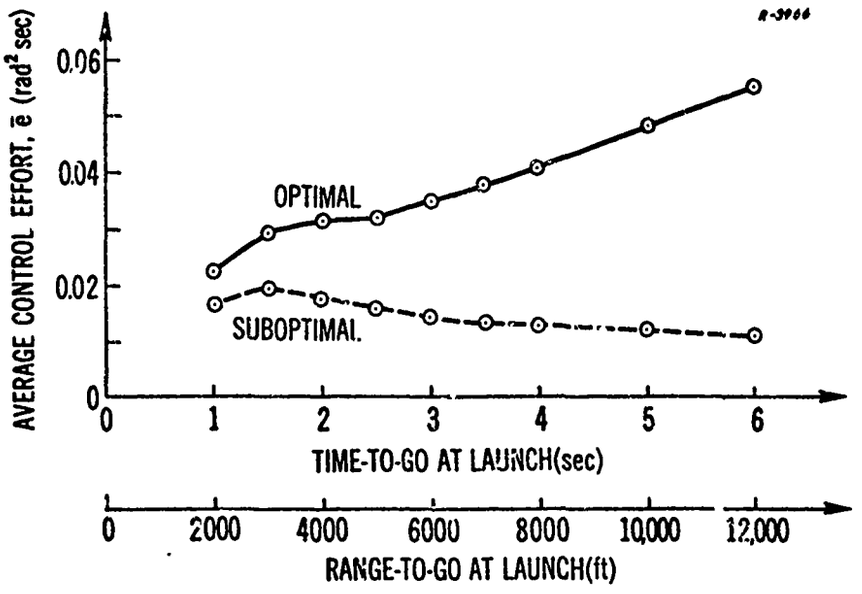

(c) Average control effort

Figure 3.2-1(cont.) Guidance Law Performance Averaged Over Twenty-Five Monte Carlo Runs: D = 0.2 rad

It has been stated that terminal miss distance is of primary importance in evaluating the guidance laws. However, because the difference between the miss distance achieved with each law is so small, other characteristics can be used as a basis of comparison. Figure 3.2-1(b) shows the rms peak airframe lateral acceleration in g's (1g = 32.2 ft/sec) encountered along each set of twenty-five trajectories. This peak acceleration usually occurs at, or just before, the terminal time, when the line-of-sight rate becomes large because of proximity to the target. Again there is little difference between the behavior of the two guidance laws. However, it is

important to note that large lateral accelerations -- in excess of 30 g's -- are developed; recall that there is nothing in the guidance problem formulation presented in Chapter 2 which directly limits acceleration. If homing sensor measurement noise or target acceleration are significantly larger than the values used for this simulation (both possibilities are realistic), lateral accelerations can be developed along the trajectory that are beyond the aerodynamic or structural capability of the missile airframe.* Consequently it will be desirable to incorporate some method of bounding acceleration within the control law; this is the subject of subsequent sections.

Another useful basis for comparing the two guidance laws is the amount of control used. Recall that the suboptimal law was derived by finding the sequence of controls which minimizes J_2 in Eq. (2.3-3). This performance index differs from that for the nonlinear law (Eq. (2.2-3)) in that it contains a term

$$r \sum_{i=0}^{N-1} u_i^2$$

which is a measure of the energy expended by some types of missile actuators in driving the control surface. To reflect this fact more clearly we define the control effort e by

$$e = \Delta t \sum_{i=0}^{N-1} u_i^2 \qquad (3.2\text{-}1)$$

The average value of e, denoted by $\bar{e}$, evaluated over each set of twenty-five Monte Carlo runs, is shown in Fig. 3.2-1(c). Evidently the suboptimal law is

*The missile airframe aerodynamic capability can be exceeded if a lateral acceleration requires an angle of attack that violates the linearity assumptions made in writing the airframe equations of motion (see Eq. (2.1-2)); the airframe structural capability is exceeded if the lateral acceleration developed by the missile causes structural failure -- e.g., if the wings are torn off.

much more efficient than the optimal law in terms of the required level of $\bar{e}$. This might be somewhat surprising because the suboptimal law was specified using a value of control weighting that can be considered equal to zero for all practical purposes; that is, the form of J_2 (with small r) is approximately the same as J_1 in Eq. (2.2-3). Consequently one might expect that the suboptimal law would be nearly identical to the optimal law; this turns out to be a false conjecture. The reason is that the control sequence $\{u_{i_0}\}$ in Eq. (2.3-16) is really a suboptimal mechanization of the linear law in Eq. (2.3-15). The latter implicitly assumes that any value of u_i can be realized at any time since no explicit constraint is imposed upon the control level. For the purpose of minimizing J_2, even as r approaches zero, it is most efficient to utilize large levels of control only near the end of the trjectory. By comparison, each time the optimal law computes a new value of u_i^o, it tries to completely null the predicted terminal miss distance $\hat{y}_{1_i}$ in Eq. (2.2-7). This tends to require larger control levels than the suboptimal law, especially during the initial portion of the trajectory. The differences between the two guidance laws are illustrated in Figs. 3.2-2 and 3.2-3 where representative gain histories and the rms control level, $|u_i|_{rms}$, are shown for trajectories initiated at six seconds before intercept.

In Fig. 3.2-2, the third elements, d_{i_3} and c_{i_3}, of $\underline{d}_i$ and $\underline{c}_i$ respectively in Eqs. (2.2-10) and (2.3-16) are plotted; the relative behavior of these two quantitives is characteristics of all the feedback gains. Observe that the optimal gain, d_{i_3}, is much larger than suboptimal gain c_{i_3} near the beginning of the trajectory. If the weighting constant r were reduced below the value ten, the effect on c_{i_3} would be a noticeable increase for small values of time-to-go but essentially no change during the earlier portion of the trajectory. In the presence of control surface limiting, the latter behavior has no appreciable effect on the terminal guidance accuracy provided by the suboptimal law.

Figure 3.2-3 compares the rms control levels (averaged over twenty-five Monte Carlo runs) for both control laws. These curves reflect

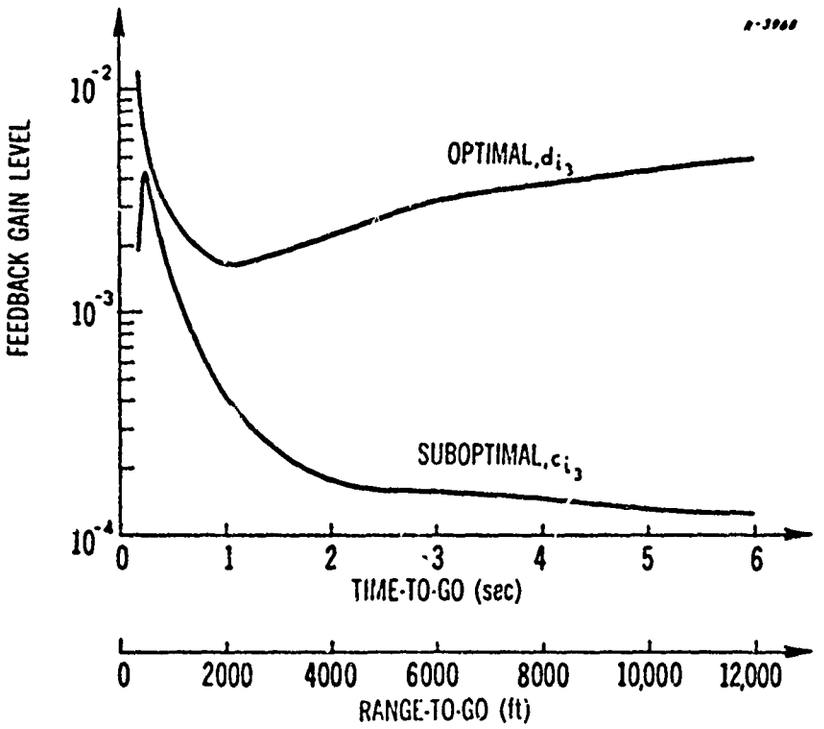

Figure 3.2-2 Representative Feedback Gain Histories for Optimal and Suboptimal Guidance Laws: Trajectories Beginning Six Seconds Before Intercept

the fact that the feedback gains for the optimal law are substantially larger, especially during the first part of the trajectory. It is also generally true that the control command frequently changes sign so that the airframe input is subjected to an input having a "bang-bang" character. This may be undesirable for applications where the missile airframe has serious bending modes that can be excited by the control switching action.

The fact that the control levels are generally larger during the first part of the missile trajectory for the optimal guidance law than they are for the suboptimal law provides a corresponding difference in the level airframe lateral acceleration. This is indicated in Fig. 3.2-4, where rms acceleration histories beginning at six seconds before intercept are plotted for both guidance laws. (This figure cannot be deduced from Fig. 3.2-1(b), which shows only rms peak acceleration). Again, there is direct evidence of the fact that the optimal law works harder, earlier, to null the terminal

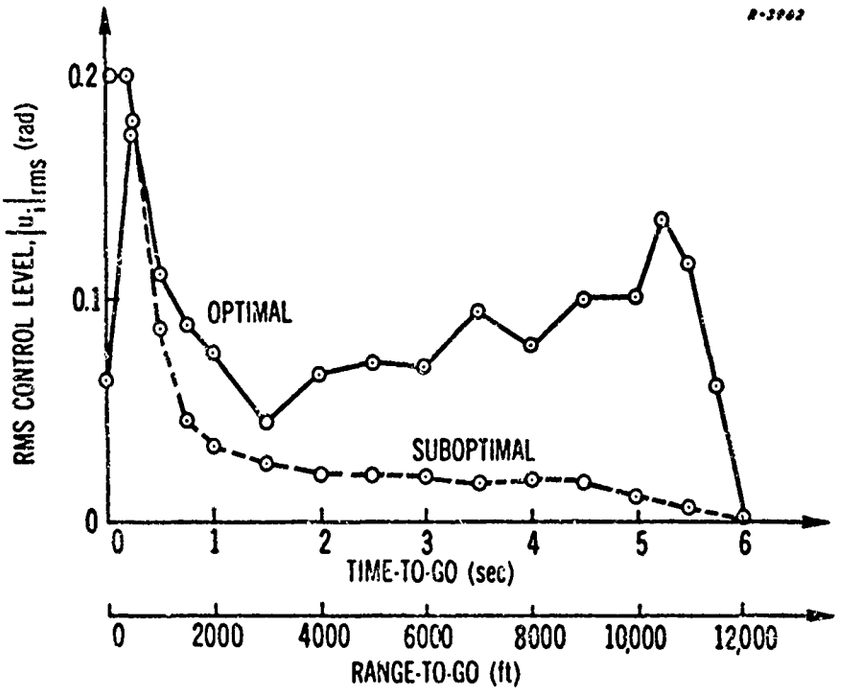

Figure 3.2-3 RMS Control Level: Trajectories Beginning Six Seconds Before Intercept

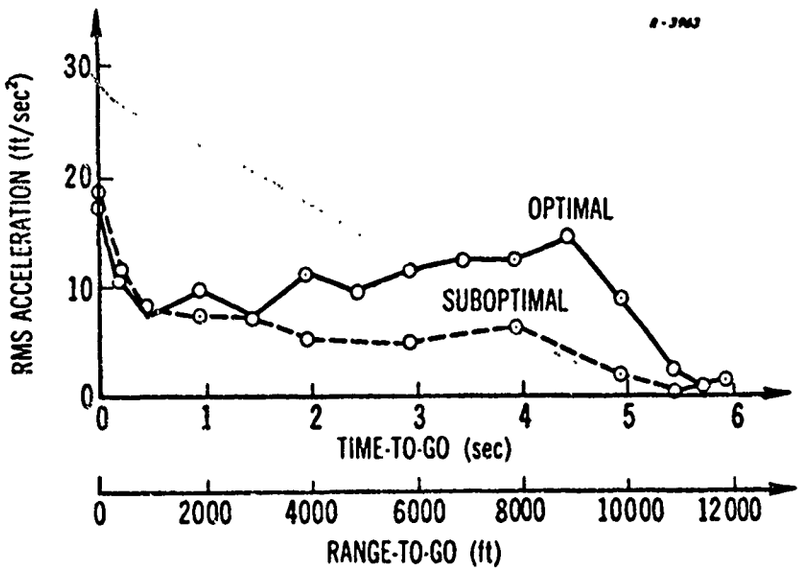

Figure 3.2-4 RMS Acceleration Level: Trajectories Beginning Six Seconds Before Intercept

miss distance. Notice also that, as mentioned previously, the peak acceleration levels for both laws occur at the end of the trajectory. One consequence of these observations is that the missile velocity losses caused by induced drag will be greater for the optimal law. This may be an important consideration, especially in long range missions or for missiles having a low lift/drag ratio.

Another interesting point to be made here is the comparison between the linear steering law given by Eq. (2.3-15) and the suboptimal nonlinear law in Eq. (2.3-16). Suppose there actually were no constraint on control surface deflection; then how well would the linear law perform? This question can be most readily answered by evaluating J_2 in Eq. (2.3-3), using the expression in Eq. (A.2-5). The latter becomes

$$J_2^o = s_0 \underline{\varphi}_0^T P_0 \underline{\varphi}_0 + \sum_{i=0}^{N-1} s_{i+1} \left(\underline{\varphi}_{i+1}^T Q_d \underline{\varphi}_{i+1} + \delta_{1_i} c_i \underline{\varphi}_i^T P_i \underline{\varphi}_i \right) \quad (3.2\text{-}2)$$

where the matrix Q_d is obtained by substituting from Eqs. (3.1-3) and (2.1-8) into Eq. (2.1-15), the matrices P_i are obtained from the Kalman filter equations (Eq. (2.2-5)), δ_{1_i} is given by Eq. (A.4-6), and c_i and s_i are determined by Eq. (2.3-14), The value of J_2^o is to be compared with the empirically determined average value of J_2, denoted by $\bar{J}_{2_o}$, obtained by using the nonlinear control sequence $\{u_{i_o}\}$ given in Eq. (2.3-16);

$$\bar{J}_{2_o} = \overline{x_1(t_f)^2} + r \overline{\sum_{i=0}^{N-1} u_{i_o}^2} \quad (3.2\text{-}3)$$

where the overbars denote averages over twenty-five Monte Carlo runs. The values of J_2^o and $\bar{J}_{2_o}$ are shown in Fig. 3.2-5 for the different launch times used in the simulations for Fig. 3.2-1. Evidently the performance predicted by the linear theory (J_2^o) is much better than that obtained when the control surface deflection constraint is imposed. This emphasizes the fact that in order to obtain a realistic indication of actual guidance accuracy, simulations must be performed with control level constraints included; analyses based exclusively upon linear theory tend to be quite inaccurate.

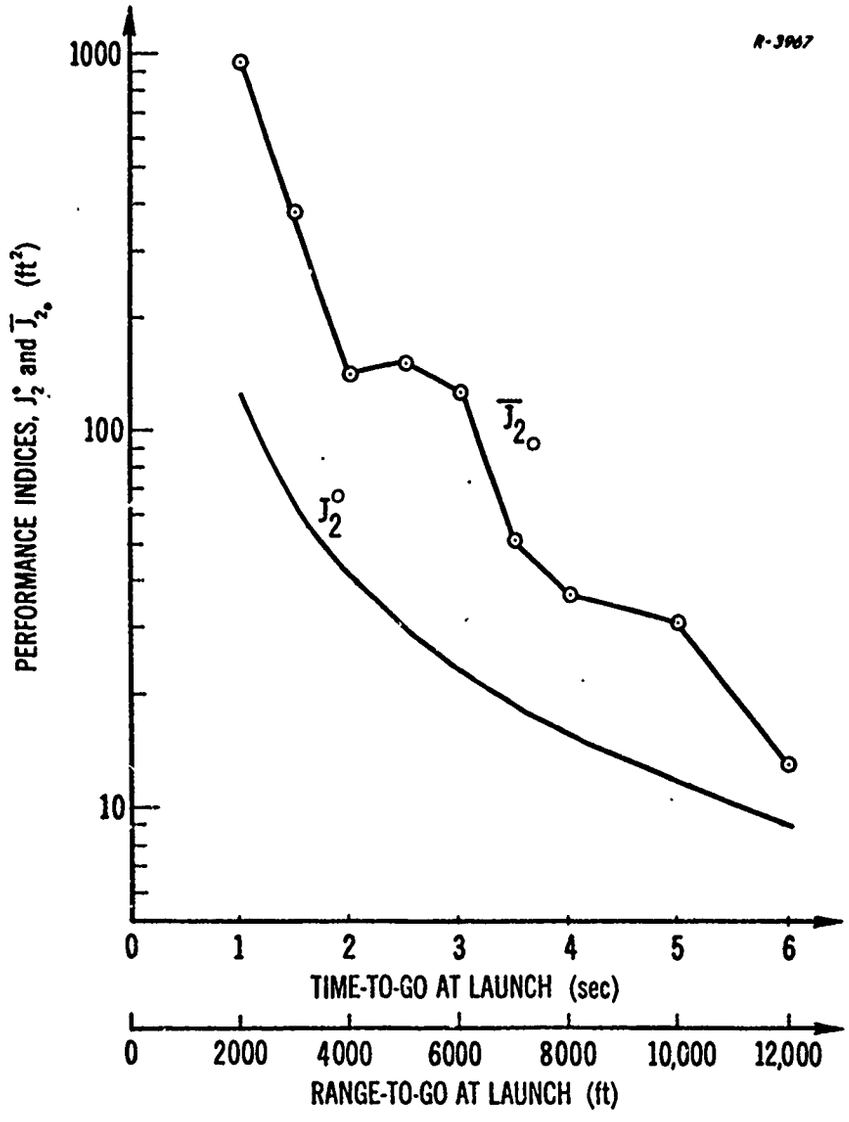

Figure 3.2-5 Values of the Quadratic Performance Index With and Without Control Surface Limiting

A number of other simulations were performed with different values assigned to various parameters -- such as homing sensor noise level, rms target acceleration, maximum control surface deflection, etc. The qualitative behavior of the data obtained is similar to that shown in Figs. 3.2-1 through 3.2-5. The conclusions reached thus far are summarized below for convenient reference:

- The terminal accuracy achieved by the optimal nonlinear guidance law is not substantially better (usually less than ten percent better) than that provided by the suboptimal technique.

- The suboptimal law uses much less control effort -- about one-tenth as much as the optimal law; the latter is bang-bang in nature, a fact that may be important when significant bending modes are present.

- The levels of rms peak airframe lateral acceleration generated by each method are approximately the same; however situations can occur where potentially unacceptable levels (thirty to ninety g's) occur.

- As pointed out in Chapter 2, the gains ($\underline{d}_i$) associated with the optimal law are more easily derived than those ($\underline{c}_i$) for the suboptimal law.

The above conclusions do not establish a definite preference for either guidance policy. A decision cannot be made between the two guidance laws on the basis of terminal accuracy because the optimal law is only slightly better in this respect. The optimal law is more easily mechanized but, against this advantage one must weigh the advantage that the suboptimal law requires lower control levels. However, one important question must be resolved before a definitive judgement can be made about either guidance technique. Namely, the simulations must account for the fact that the maneuvering acceleration available is limited by physical constraints in any practical application. For the case considered here -- i.e., a missile using aerodynamic lift to develop maneuvering force -- some method of preventing each guidance law from developing excessive airframe lateral acceleration must be provided. Consequently, the remainder of this chapter is concerned with methods for limiting acceleration. This investigation will lead to more distinctive comparisons between guidance laws.

3.3 A PREDICTIVE ACCELERATION LIMITER

The most straightforward approach for limiting airframe lateral acceleration is to include a constraint of the form

$$E\left\{|a_m(t)|\right\} \leq D_a$$

in the design criteria for the guidance problem, where D_a is the maximum permissible acceleration. This type of "state variable constraint" can easily be included within the framework of the problem formulated in Section A.3. However, the simplifications described in Section A.4 which allow the optimal controls to be derived analytically cannot be applied. Consequently the control law must be computed numerically, a task that is currently impractical to accomplish. Therefore we must settle for some other technique to constrain acceleration.

Another approach that could be taken is to artificially limit the control surface deflection, u_i, at some value which physically tends to prevent large accelerations from being generated. For example, guidance law performance data are given in Fig. 3.3-1 with the same simulation parameter values used in Section 3.2, except that the value of D is reduced from 0.2 to 0.1 radian. Comparing these results with Figs. 3.2-1(a) and (b), we find a general increase in the level of rms terminal miss distance and a corresponding decrease in the rms peak acceleration. However, this method of effecting a reduction in acceleration tends to be excessively conservative. Intuitively it seems desirable to restrict $|u_i|$ only when the airframe acceleration approaches the danger level; when it is well within the safe operating limits, the maximum available control surface deflection should be allowed. This reasoning leads us to seek a more efficient method for limiting acceleration; one such technique is presented in this section.

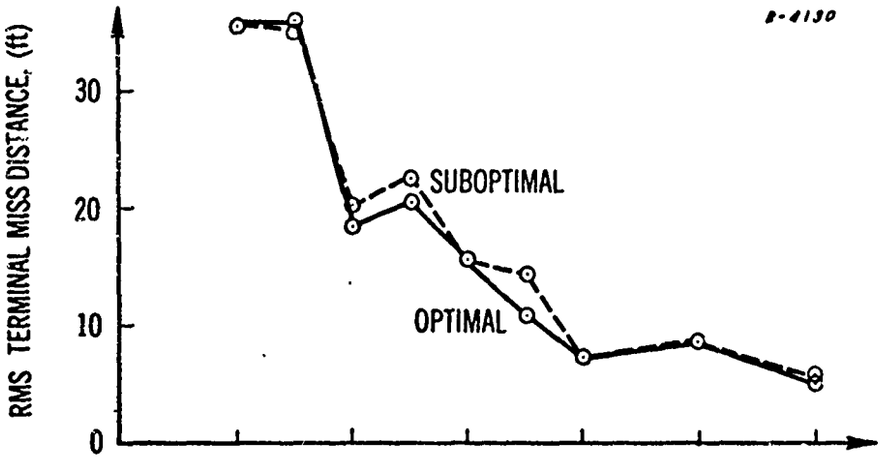

(a) rms terminal miss distance

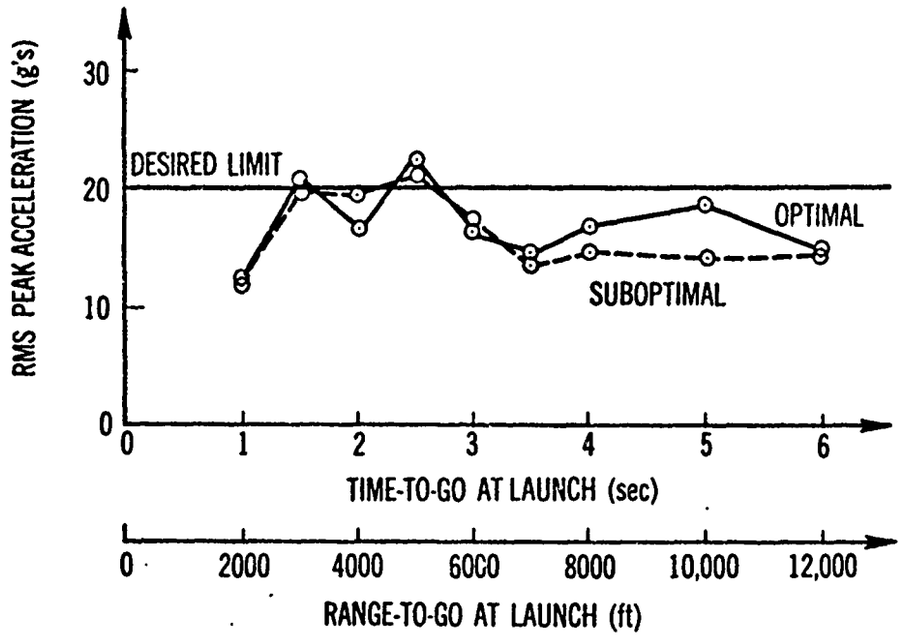

(b) rms peak lateral acceleration

Figure 3.3-1 Guidance Law Performance Averaged Over 25 Monte Carlo Runs: D = 0.1 rad

Suppose a value of control surface deflection, u_i, is computed at time t_i by either one of the procedures given in Eqs. (2.2-10) and (2.3-16). We wish to determine whether to apply u_i to the airframe or to take some other action that will limit the buildup in lateral acceleration. At time t_i an estimate, $\hat{\underline{x}}_i$, of the state of the guidance system is also available from the Kalman filter, based on previous measurements and applied controls. In order to arrive at an appropriate decision about implementing u_i, the predicted acceleration level at some specified future time, $t_i + \tau_p$, caused by $\hat{\underline{x}}_i$ and the control u_i is computed and compared against the desired bound, D_a. If the predicted acceleration is too large, u_i should be altered to prevent the bound from being exceeded. A procedure for carrying out this policy is described below.

For a prediction interval of variable length τ, the predicted state, $\hat{\underline{x}}(t_i+\tau)$, satisfies a differential equation similar to Eq. (2.1-7);

$$\frac{d}{d\tau}\left[\hat{\underline{x}}(t_i+\tau)\right] = F\,\hat{\underline{x}}(t_i+\tau) + \underline{g}\,u(t_i+\tau)$$

$$u(t_i+\tau) = \begin{cases} u_i\,; & 0 \le \tau < \Delta t \\ 0\,; & \Delta t \le \tau \end{cases} \qquad (3.3\text{-}1)$$

where $u(t)$ is assumed to be zero after the application of u_i. Therefore $\hat{\underline{x}}(t_i+\tau)$ is given by

$$\hat{\underline{x}}(t_i+\tau) = e^{F\tau}\,\hat{\underline{x}}(t_i) + \int_{t_i}^{t_i+\tau} e^{F(t_i+\tau-\lambda)}\,\underline{g}\,u(\lambda)\,d\lambda$$

where $e^{F\tau}$ is the matrix exponential series for $F\tau$; it is also the transition matrix $\Phi(\tau,0)$ given analytically by Eqs. (2.2-12) and (2.2-13). Assuming that $\tau > \Delta t$ and recognizing that $u(t_i+\tau) = 0$ when $\tau > \Delta t$ we have

$$\hat{\underline{x}}(t_i+\tau) = e^{F\tau}\hat{\underline{x}}(t_i) + \int_0^{\Delta t} e^{F(\tau-\lambda)}\,\underline{g}u_i\,d\lambda$$

$$= e^{F\tau}\left[\hat{\underline{x}}(t_i) + \int_0^{\Delta t} e^{-F\lambda}\,\underline{g}u_i\,d\lambda\right]$$

$$= e^{F\tau}\left[\hat{\underline{x}}(t_i) + e^{-F\Delta t}\int_0^{\Delta t} e^{F(\Delta t-\lambda)}\,\underline{g}u_i\,d\lambda\right] \qquad (3.3\text{-}2)$$

Comparing the last equality in Eq. (3.3-2) with Eq. (2.1-14) and setting $\tau = \tau_p$, a specified interval, we see that

$$\hat{\underline{x}}(t_i+\tau_p) = e^{F\tau_p}\hat{\underline{x}}(t_i) + e^{F(\tau_p-\Delta t)}\,\underline{\gamma}u_i$$

$$= \Phi(\tau_p, 0)\,\underline{x}(t_i) + \Phi(\tau_p-\Delta t, 0)\,\underline{\gamma}u_i \qquad (3.3\text{-}3)$$

Now because missile acceleration due to lift is the n^{th} state variable in Eq. (2.1-6), let $\underline{\eta}$ be a column vector formed from the bottom row of $\Phi(\tau_p, 0)$ and let η_o be the last element of the vector $\Phi(\tau_p - \Delta t, 0)\,\underline{\gamma}$. Then if $\tau_p > \Delta t$, it follows that the predicted airframe lateral acceleration, $\hat{a}_m(t_i+\tau_p)$, is given by

$$\hat{a}_m(t_i+\tau_p) = \underline{\eta}^T\hat{\underline{x}}_i + \eta_o u_i \qquad (3.3\text{-}4)$$

Once the prediction interval τ_p is selected, $\underline{\eta}$ and η_o can be computed from knowledge of both the transition matrix and the vector $\underline{\gamma}$ and programmed into the guidance controller as constant gains, or possibly as time-varying gains if the parameters defining the transition matrix vary in a known manner.*

Having the predicted acceleration, we can determine whether its magnitude exceeds the specified bound, D_a. If it does, the value of u_i should be modified to reduce $|a(t_i + \tau_p)|$, taking care to ensure that $|u_i|$ does not exceed the control surface deflection limit D. This sequence of logical tests is accomplished with the aid of Eq. (3.3-4) as follows:

$$u_i = \begin{cases} u_i^o & ; \quad \text{Optimal Law} \\ u_{i_o} & ; \quad \text{Suboptimal Law} \end{cases}$$

$$u_i' = \begin{cases} u_i \ ; & D_a - |\hat{a}_m(t_i+\tau_p)| \geq 0 \\ \left[D_a \ \text{sgn}\left[\hat{a}_m(t_i+\tau_p)\right] - \underline{\eta}^T \hat{\underline{x}}_i\right]/\eta_o & \\ \text{or equivalently} & D_a - |\hat{a}_m(t_i+\tau_p)| < 0 \\ u_i - \left\{\hat{a}_m(t_i+\tau_p) - D_a \ \text{sgn}\left[\hat{a}_m(t_i+\tau_p)\right]\right\}/\eta_o & \end{cases}$$

$$u_i'' = \begin{cases} u_i' & ; \quad D - |u_i'| \geq 0 \\ D \ \text{sgn}(u_i'); & D - |u_i'| < 0 \end{cases} \qquad (3.3\text{-}5)$$

*Again we note that if the missile airframe dynamics are identified on line, then the analytical expressions for $\underline{\eta}$ and η_o must be stored and evaluated on-line as parameters are identified.

The quantity u_i' is generated to reduce the level of predicted acceleration if the latter is too large. The resulting level of u_i' required to correct the acceleration could exceed the control surface deflection limits; this possibility is prevented by calculating u_i'' which is the new control surface deflection command. The operations are illustrated in Fig. 3.3-2.

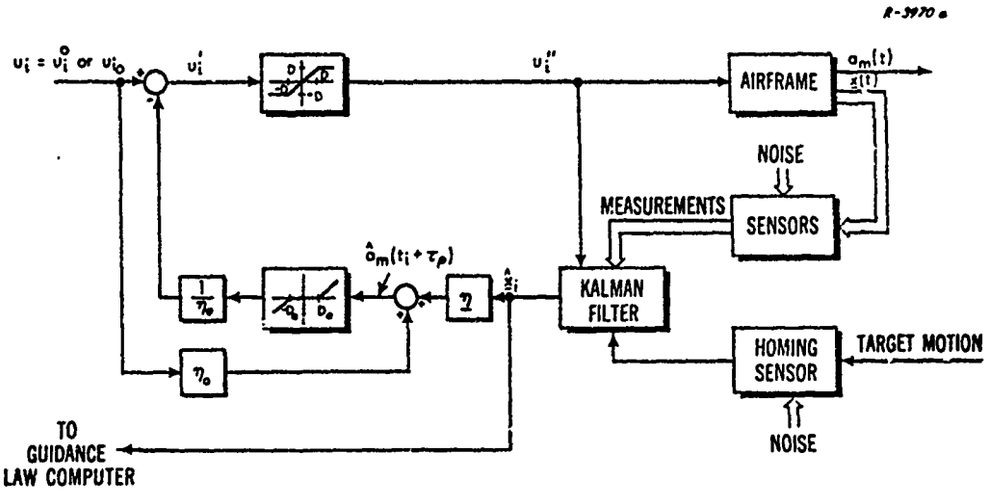

Figure 3.3-2 Mechanization of the Predictive Acceleration Limiter

It is emphasized that the method described above for limiting airframe lateral acceleration is not necessarily an optimal procedure, although it is a physically reasonable one. The choice of the prediction interval τ_p is somewhat subjective. If it is too small, the airframe acceleration may overshoot the bound; if it is too large, limiting action may occur before it is actually necessary. In these simulations, $\tau_p = 0.2$ sec was found to be satisfactory.

To implement the acceleration limiter represented by Eq. (3.3-5), the quantities -- D_a, $\underline{\eta}$ and η_o -- are needed. The airframe structural limits dictate the value of D_a; $\underline{\eta}$ and η_o are specified by the transition matrix, $\exp(F\tau_p)$, according to Eqs. (3.3-3) and (3.3-4). The computation required for the limiter is a minor part of the total needed to generate the control commands.

3.4 SIMULATION RESULTS WITH ACCELERATION LIMITING

In this section, results are presented from a number of different Monte Carlo simulations of the guidance laws derived in Chapter 2, when the predictive acceleration limiter defined in the preceeding section is used. Because the limiting procedure is not necessarily optimal, the control sequences actually applied as a result of either guidance laws are probably suboptimal. They are derived by operating on $\{u_i^o\}$ and $\{u_{i_o}\}$ respectively, from Eqs. (2.2-10) and (2.3-16), with the logical tests given in Eq. (3.3-5). The resulting sequences are designated as $\{u_{i_o}^o\}$ and $\{u_{i_{oo}}\}$. This notation is suggestive of the fact that the former is suboptimal only in its treatment of acceleration limiting; the latter is suboptimal with respect to both control level and acceleration level limiting. For the reader's convenience, the four guidance laws we have derived are summarized below:

$\{u_i^o\}$: Optimal Nonlinear Guidance Law; minimizes terminal miss distance subject to bounded control level. No explicit acceleration constraint imposed.

$\{u_{i_o}\}$; Suboptimal Nonlinear Guidance Law; derived using "linear quadratic gaussian theory" and imposing the control bound after the fact. No explicit acceleration constraint imposed.

$\{u^o_{i_o}\}$; Suboptimal Law; derived by operating on $\{u^o_i\}$ with an acceleration limiter.

$\{u_{i_{oo}}\}$; Suboptimal Law; derived by operating on $\{u_{i_o}\}$ with an acceleration limiter.

Each guidance law was evaluated for the five cases given in Table 3.4-1. Under each case, twenty-five Monte Carlo simulations were performed for each of nine cases having launch times of one through six seconds before intercept, the same launch times used in the simulations described in preceding sections. A number of parameters were held fixed for all cases; these are:

Control Weighting:	$r = 10\ ft^2/rad^2$
RMS Measurement Noise:	$r_{22} = 5.0 \times 10^{-6} (rad/sec)^2$
	$r_{33} = 10\ (ft/sec^2)^2$
	$r_{ij} = 0; \quad i \neq j$
Initial State Covariance Matrix:	$p_{11} = 0$
	$p_{22} = 0$
	$p_{44} = 1.0 \times 10^{-4} (rad/sec)^2$
	$p_{55} = 1.0 \times 10^{3} (ft/sec^2)^2$
	$p_{ij} = 0; \quad i \neq j$
Control Surface Deflection Limit:	$D = 0.2$ radian
Lateral Acceleration Limit:	$D_a = 20$ g's
Mean Value of Initial State:	$\underline{\mu} = \underline{0}.$

TABLE 3.4-1

TRAJECTORY SIMULATION PARAMETER VALUES

Simulation Parameter	Case Number				
	1 Standard	2 Lower Missile Airspeed	3 Smaller Target Time Constant	4 Larger Homing Sensor Noise	5 Higher rms Target Acceleration
M_q	- 0.455	- 0.31	- 0.455	- 0.455	- 0.455
M_α	- 8.4	- 7.05	- 8.4	- 8.4	- 8.4
M_δ	-71.2	-47.0	-71.2	-71.2	-71.2
L_α	10.15	7.27	10.15	10,15	10.15
L_δ	1.86	2.15	1.86	1.86	1.86
V	2920	1920	2920	2920	2920
f_t	- 0.3	- 0.3	- 0.1	- 0.3	- 0.3
σ_s	4.75	4.75	4.75	15.0	4.75
p_{33}	9.0×10^3	9.0×10^3	9.0×10^3	9.0×10^3	3.6×10^4
v_c	2000	1000	2000	2000	2000
σ^2	9.0×10^3	9.0×10^3	9.0×10^3	9.0×10^3	3.6×10^4
Δt	0.05	0.05	0.05	0.05	0.05

Case number 1 in Table 3.4-1 is referred to as the standard; its parameter values are the same as those used in the simulation described in Section 3.2 except that acceleration limiting has been added. The other four cases are described relative to the standard -- e.g., lower missile airspeed, smaller target time constant, etc.

The performance data for case 1 are displayed in Fig. 3.4-1, which is to be compared with Fig. 3.2-1. In general the miss distances for both guidance laws are now larger because the missile's maneuvering

capability has been restricted. However a more significant observation is that the rms terminal miss distance (see Fig. 3.4-1(a)) achieved with $\{u_{i_o}^o\}$ is significantly lower -- as much as thirty percent lower -- than that obtained with $\{u_{i_{oo}}\}$. Thus when acceleration limiting is introduced into the guidance laws derived in Chapter 2, the performance advantage of the optimal law improves. The improvement is even greater when the levels of measurement noise and/or target acceleration are increased, as will be seen from the results of the other cases in Table 3.4-1. To understand why this improvement in relative performance of the optimal nonlinear law occurs, recall that when the acceleration limiter is absent each new value of u_i^o attempts to null the predicted terminal miss calculated at the i^{th} stage. On the other hand, the suboptimal nonlinear controls $\{u_{i_o}\}$ tend to reduce the terminal miss distance more gradually. These different control actions cause the lateral acceleration history for $\{u_i^o\}$ to have a larger magnitude than that for $\{u_{i_o}\}$ until near the end of the trajectory (see Fig. 3.2-4). For both guidance laws, the acceleration levels become largest near the end of the trajectory, because large accelerations are needed to null miss distance when there is little time remaining until intercept. Now, when acceleration limiting is introduced, the sequence $\{u_{i_o}^o\}$ has an advantage over $\{u_{i_{oo}}\}$. The former, because it is derived from the optimal nonlinear law, makes an effort to null the terminal miss early in the trajectory where less lateral acceleration is required than if it waits until near the intercept point. Consequently, as the intercept point is approached $\{u_{i_o}^o\}$ has, on the average, already significantly reduced the terminal miss. By comparison, $\{u_{i_{oo}}\}$, because it is derived from the suboptimal nonlinear law from Chapter 2, does relatively little controlling early in flight; therefore as the intercept point is approached a relatively large terminal miss remains to be nulled. Consequently, the acceleration limiter, which applies limiting action primarily near the end of the

trajectory, tends to degrade the performance of $\{u_{i_{OO}}\}$ less than that of $\{u^o_{i_o}\}$. These observations suggest that the control sequence $\{u^o_{i_o}\}$ may be close to optimal in the presence of acceleration limiting. However, this conjecture can be verified only by actually determining the control law that minimizes the magnitude of the terminal miss subject to constraints on both control and acceleration levels, as suggested at the beginning of Section 3.3.

There is a property of the acceleration limiter that can degrade the performance of $\{u^o_{i_o}\}$ relative to $\{u_{i_{OO}}\}$. If the homing sensor measurement noise causes an inaccurate estimate of the terminal miss distance several seconds before intercept, then the corresponding applied control $u^o_{i_o}$ may correct the missile's trajectory in the wrong direction. If this happens, the other control law is preferred because it tends to apply less "wrong control" early in the trajectory. Fortunately, this effect apparently does not occur sufficiently often to contribute significantly to the rms performance data in Fig. 3.4-1(a); however, it can show up in individual trajectories.

Figure 3.4-1(b), compared with Fig. 3.2-1(b), indicates that the limiter is successful in reducing the rms peak acceleration below the bound of twenty g's. As expected, the limiting action causes the absolute values of miss distance to increase (compare Figs. 3.4-1(a) and 3.2-1(a)). However, note that the predictive limiter generally achieves lower miss distances than the technique of artificially reducing the bounds on control surface deflection demonstrated in Fig. 3.3-1.

In order to provide an additional indication of the amount of control required for each guidance law, we define the control variation, v,

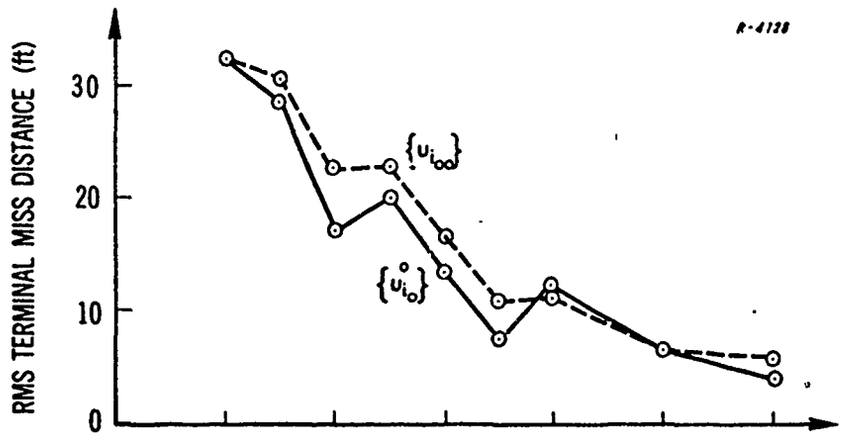

(a) Miss distance

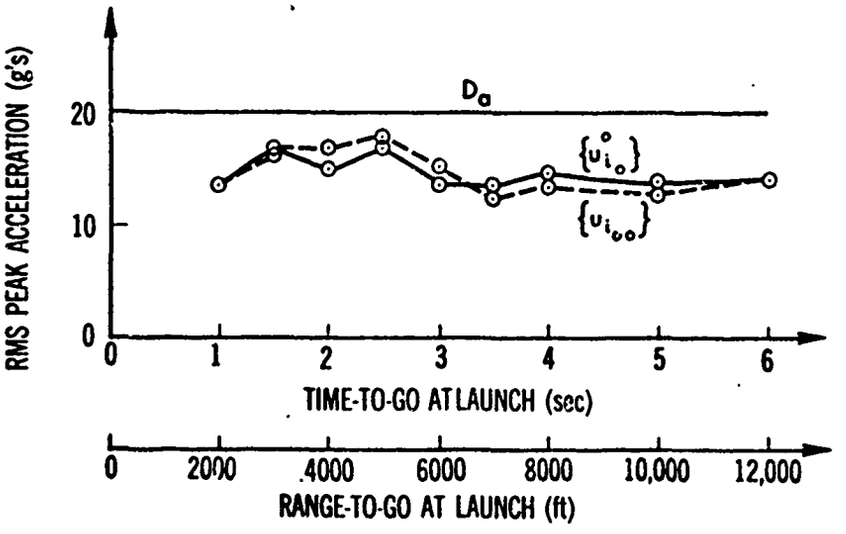

(b) Acceleration

Figure 3.4-1 **Performance Evaluation of Suboptimal Guidance Laws Including Acceleration Limiting: Case 1**

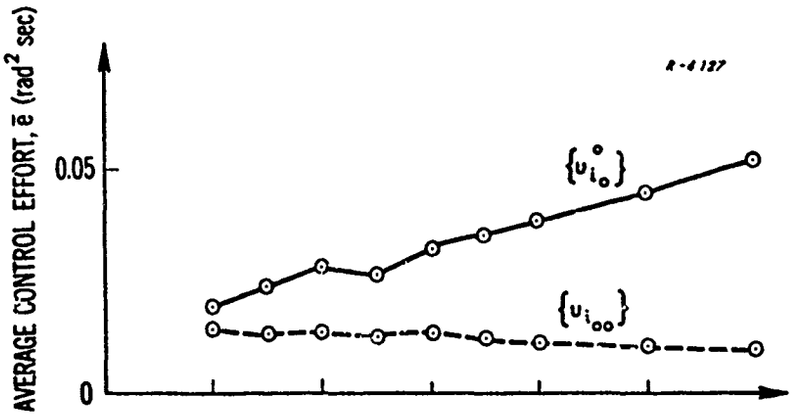

(c) Average control effort

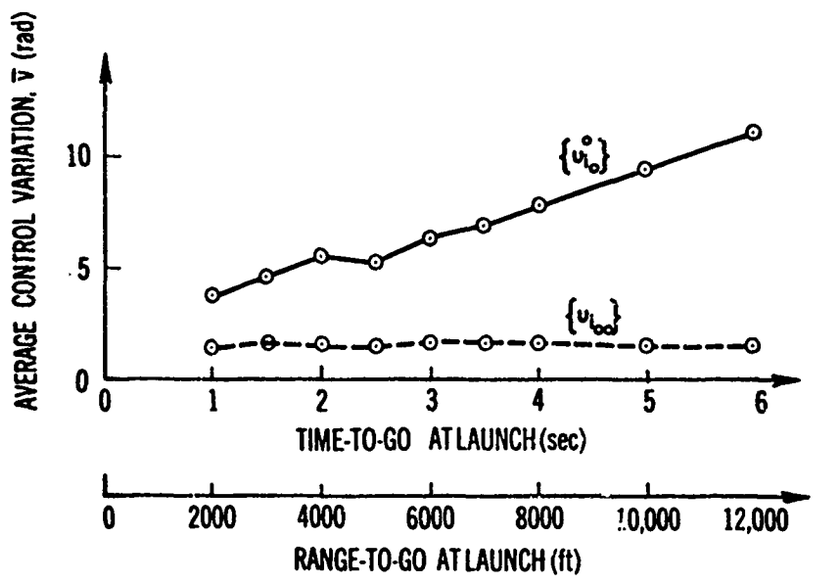

(d) Average control variation

Figure 3.4-1(cont.) Performance Evaluation of Suboptimal Guidance Laws Including Acceleration Limiting: Case 1

$$v = |u_0| + \sum_{i=0}^{N-2} |u_{i+1} - u_i| \qquad (3.4\text{-}1)$$

In some missiles v is a more accurate measure of the actuator energy expenditure than is the control effort e in Eq. (3.2-1), particularly when an electrohydraulic actuator mechanism is employed which consumes power only when the control surface deflection is changing. In addition, in some hydraulic systems a change in control level is achieved by movement of fluid which is discharged overboard. In the latter case, v represents the amount of fluid consumed. The average value, $\bar{v}$, of the control level variation, evaluated over each set of twenty-five Monte Carlo runs, is displayed in Fig. 3.4-1(d).

The data presented for both $\bar{e}$ and $\bar{v}$ in Figs. 3.4-1(c) and (d) indicate that the control sequence $\{u_{i_0}^o\}$ demands significantly more actuator energy than does $\{u_{i_{oo}}\}$, particularly for large launch ranges. This observation is consistent with the behavior of $\bar{e}$ in Fig. 3.2-1. The high level of $\bar{v}$ is a result of the fact that the control action is quasi bang-bang in nature; that is, $u_{i_0}^o$ tends to change sign frequently.

The levels of $\bar{e}$ and $\bar{v}$ required for $\{u_{i_{oo}}\}$ remain fairly constant as the launch time increases; however, the curves for $\{u_{i_0}^o\}$ increase with launch time. This behavior can be expected from the gain histories $\underline{c}$ and $\underline{d}$ associated with each law which are illustrated in Fig. 3.2-2. For long trajectories $\{u_{i_{oo}}\}$ may be preferred, at least until the missile is close enough to the target so that sufficient control surface actuation capability remains to permit the use of $\{u_{i_0}^o\}$. Thus some type of dual-mode guidance laws discussed in this report may be desirable. There are a variety of methods one could use to accomplish this; the particular one selected would be strongly dependent upon the type of mission -- i.e., long-range

or short-range -- under consideration. This is a subject which merits further investigation.

In presenting performance data for the other cases given in Table 3.4-1, only the rms terminal miss distance and peak acceleration are displayed. In all cases the behavior of $\bar{v}$ and $\bar{e}$ is qualitatively the same as in Fig. 3.4-1.

Case 2 in Table 3.4-1 is characterized, relative to Case 1, by a lower missile airspeed, V. This change also affects other parameters -- namely the airframe stability derivatives, which are dependent upon Mach number, and the closing velocity. For the particular airframe data used here, the decrease in V alters the airframe dynamics so that the control surface effectiveness is reduced and the distance between the airframe-wing center of pressure and the missile center of gravity is increased. This reduces the airframe capability to generate lift (lateral acceleration) and tends to cause an increase in the miss distance compared with Case 1. On the other hand, if we assume that the closing velocity is reduced by the same amount as the airspeed, then for a given launch range, the total number of measurements taken over the entire trajectory increases. Consequently, more averaging of measurement errors is performed by the Kalman filter in the guidance controller, giving potentially better estimates of the system state variables. Thus a decrease in closing velocity may tend to reduce miss distance.

For the particular parameter values in Case 2, the adverse effect on miss distance produced by the changes in airframe dynamics dominates any improvement obtained with a smaller closing velocity, as seen by comparing Figs. 3.4-1(a) and 3.4-2(a) at the same values of launch range. The reduction in the airframe's ability to generate lateral acceleration is evident from a comparison of Figs. 3.4-1(b) and 3.4-2(b).

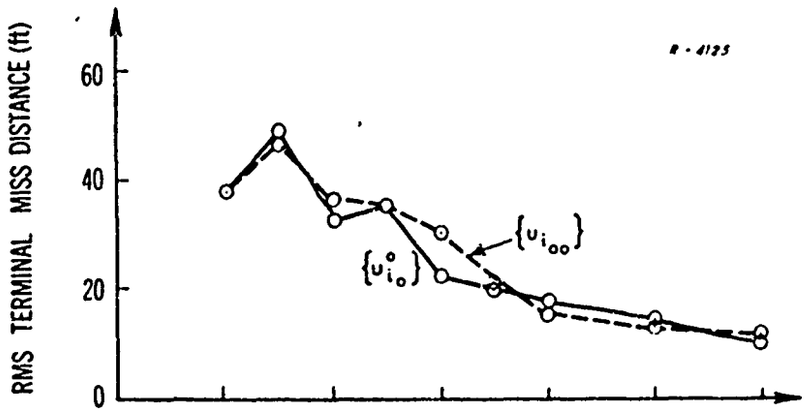

(a) Miss distance

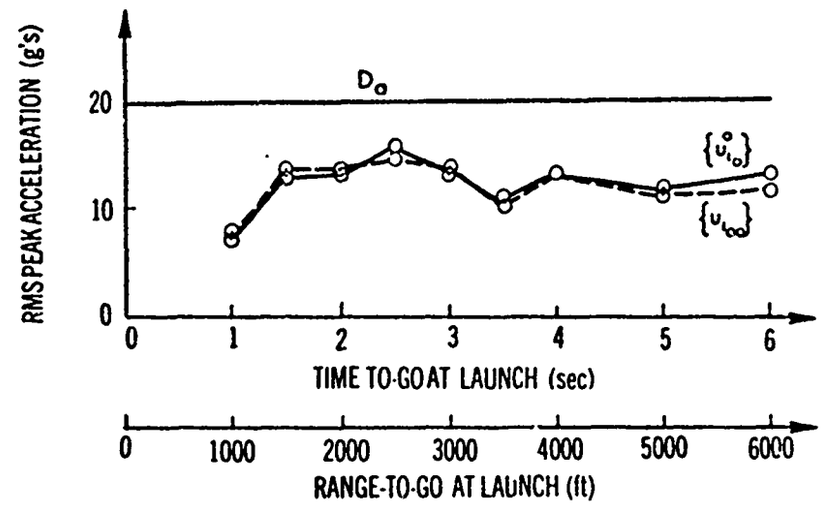

(b) Acceleration

Figure 3.4-2 **Performance Evaluation of Suboptimal Guidance Laws Including Acceleration Limiting: Case 2**

The effect of increasing the target time constant ($1/f_t$) is illustrated by Case 3 in Table 3.4-1. This change implies that the target acceleration changes more slowly than in Case 1. The effect on the guidance system is that the Kalman filter can track the target acceleration more accurately because it is more nearly constant. Consequently, with all other parameter values being unchanged, the miss distance for Case 3 should be somewhat smaller than for Case 1. This expectation is verified by comparison of Figs. 3.4-1(a) and 3.4-3(a).

The effect of an increase in the homing sensor measurement noise level is demonstrated by Case 4 where the target dimension parameter, σ_s, is increased to 15 feet. Recall that σ_s represents the average distance normal to the line-of-sight between reflecting points in the target. The effect of this change is to increase the value of r_{11} by a factor of ten. Evidently, comparing Figs. 3.4-1(a) and 3.4-4(a), much larger miss distances are incurred for both guidance laws; however, the difference between the performance of $\{u_{i_0}^o\}$ and $\{u_{i_{oo}}\}$ increases. The former yields an rms miss distance that is as much as fifty percent less than that provided by $\{u_{i_{oo}}\}$. It is also noted, comparing Figs. 3.4-1(b) and 3.4-4(b), that larger acceleration levels are needed; these are attribited to the increased rms error in estimating the guidance state variables.

Finally, Case 5 represents the effect of an increase in rms target acceleration, σ, from about 3 g's to about 6 g's. The corresponding effect on terminal miss distance and lateral acceleration is shown in Fig. 3.4-5. Relative to Case 1, the miss distance increases for both guidance laws; however, there is a widening of difference between the performance of $\{u_{i_0}^o\}$ and $\{u_{i_{oo}}\}$. The required lateral acceleration levels also increase for both guidance laws.

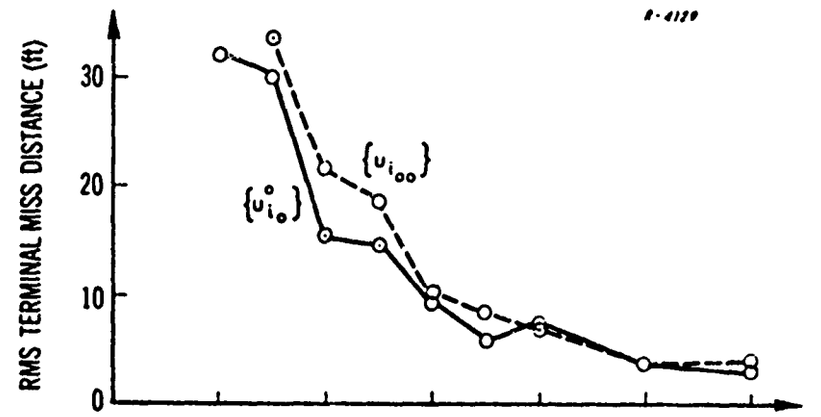

(a) Miss distance

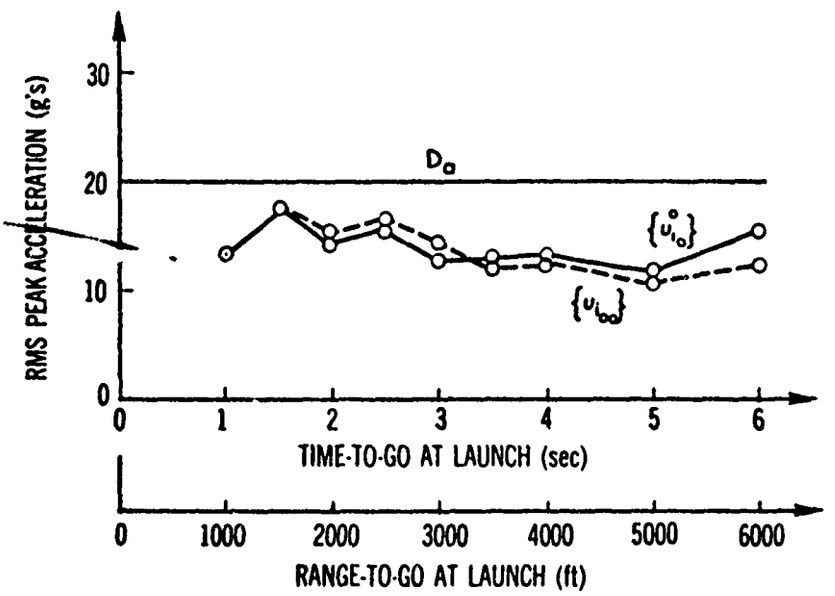

(b) Acceleration

Figure 3.4-3 **Performance Evaluation of Suboptimal Guidance Laws Including Acceleration Limiting: Case 3**

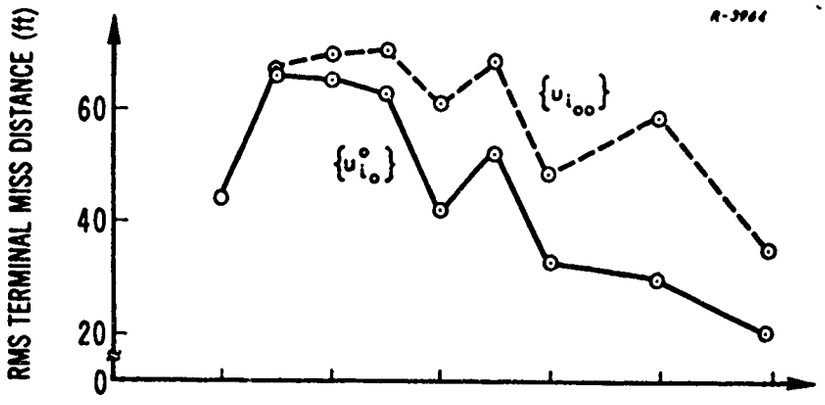

(a) Miss distance

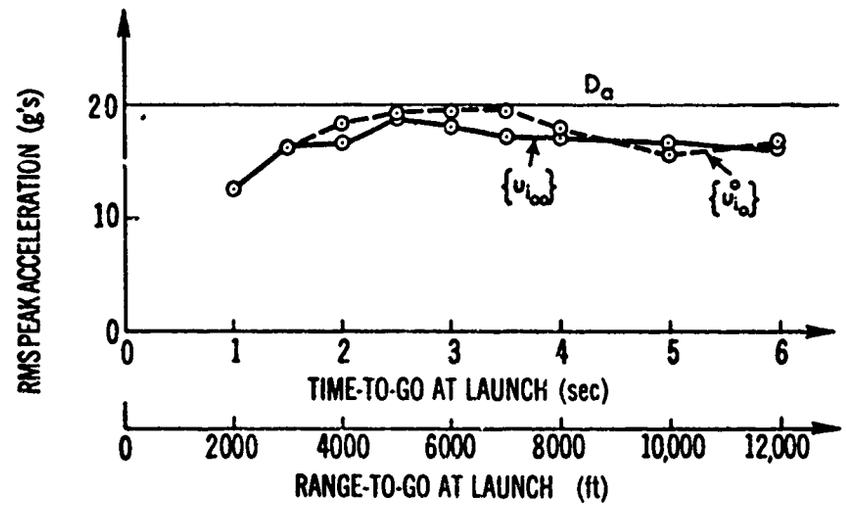

(b) Acceleration

Figure 3.4-4 Performance Evaluation of Suboptimal Guidance Laws Including Acceleration Limiting: Case 4

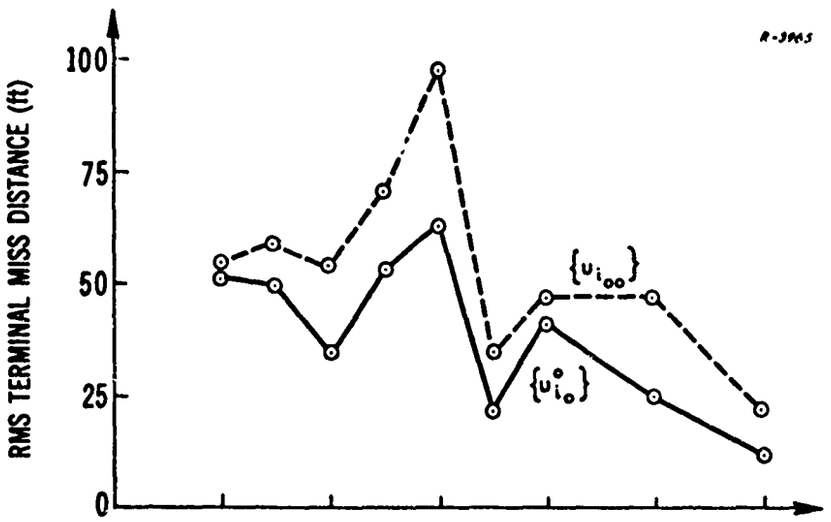

(a) Miss distance

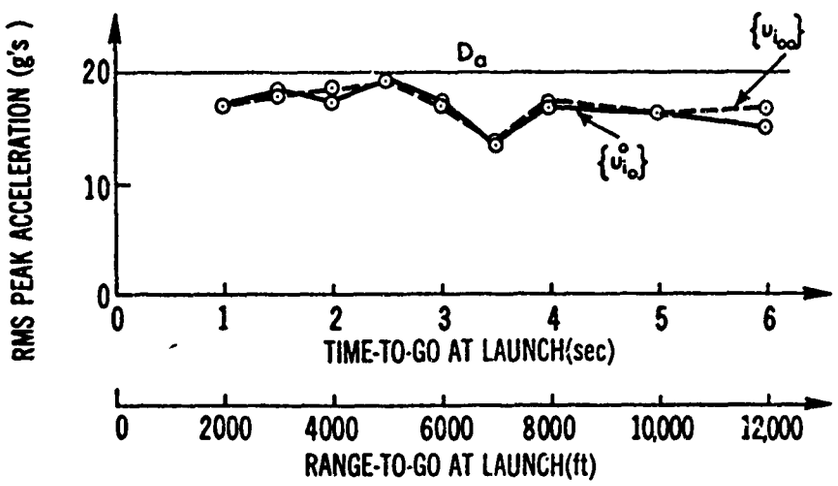

(b) Acceleration

Figure 3.4-5 **Performance Evaluation of Suboptimal Guidance Laws Including Acceleration Limiting: Case 5**

Summary – This section (3.4) has presented an evaluation of the guidance laws derived in Chapter 2, modified with the predictive acceleration limiter described in Section 3.3. In all simulations it is found that the limiter successfully maintains the rms acceleration level below the prescribed bound. In addition, the terminal miss distance achieved with $\{u_{i_o}^o\}$ is as much as fifty percent less than that produced by $\{u_{i_{oo}}\}$. This comparison substantially reverses the conclusion in Section 3.2 that the optimal nonlinear guidance law (without acceleration limiting) offers insignificant improvement over the suboptimal law. The amount of control energy, as measured by either the "effort" $\bar{e}$ or the "variation" $\bar{v}$ required, is much greater for $\{u_{i_o}^o\}$ than it is for $\{u_{i_{oo}}\}$; this difference becomes more pronounced the further the missile is from the target at the beginning of the homing guidance phase. Although we have stated that terminal miss distance is the primary basis for comparing guidance laws, the control energy requirements cannot be ignored. In some applications it may be advisable to combine the advantages of each guidance law in one dual-mode technique.

The mathematical model used here to evaluate guidance laws is sufficiently realistic to indicate that the optimal guidance law derived in Chapter 2 can offer substantial performance benefits over suboptimal laws derived by minimizing a quadratic performance index, when acceleration limiting is required. To obtain a better knowledge of performance capability, homing sensor noise models with time-varying statistics should be investigated. In addition, sensitivity studies should be made to determine the amount of performance degradation caused by inaccurate modeling of the guidance dynamics and by the intentional use of more simplified (e.g., constant gain) control laws. These topics will be the subject of further study.

4. SUMMARY AND CONCLUSIONS

4.1 SUMMARY

This report is concerned with guidance laws for tactical missiles which account for the presence of random target acceleration, homing sensor measurement errors, a constraint on the maximum control level and a constraint on the maximum airframe lateral acceleration. Emphasis is placed upon those techniques which can potentially be applied in practical tactical missile weapons systems in the next ten to twenty years, especially those which can take advantage of the rapid improvement in computer hardware technology. The particular missile considered for this investigation has an aerodynamically controlled airframe with fixed wings and tail-mounted control surfaces. However, the conclusions obtained here apply to other types of missiles as well.

In Chapter 2 the tactical missile guidance problem is formulated in the context of optimal stochastic control theory and two different guidance laws are derived, each being associated with somewhat different problem formulations. An optimal nonlinear guidance law is determined which minimizes the expected value of the squared terminal miss, subject to a constraint on the missile control surface deflection angle. This law results in the sequence of optimal control commands designated as $\{u_i^o\}$. The other guidance law is one which minimizes the expected value of a weighted sum of the squared terminal miss distance and a quadratic penalty on the control; in this case the control level limit is ignored in deriving the optimal control sequence. Then the latter is passed through a limiter which "clips" the excess control magnitude resulting in a suboptimal nonlinear guidance law represented by $\{u_{i_o}\}$.

Simulations of both of the above mentioned guidance laws are described in Chapter 3. It was found that both laws tend to call for large

airframe lateral accelerations that could be excessive in some practical applications. Consequently a predictive acceleration limiter was devised for modifying each control sequence to prevent excessive acceleration build-up; this procedure is described in Section 3.3. The modified control sequences are designated as follows:

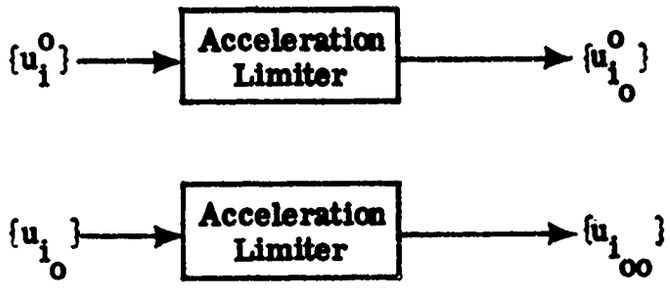

The sequences $\{u_{i_o}^o\}$ and $\{u_{i_{oo}}\}$ are regarded as two additional suboptimal nonlinear guidance laws; they are both suboptimal because the limit on acceleration has been imposed "after the fact," rather than being part of the guidance law design criterion. To further aid in distinguishing the guidance laws, it is useful to define the following two categories of sequences of control commands:

Type I Laws	Type II Laws
$\{u_{i_o}\}$	$\{u_i^o\}$
$\{u_{i_{oo}}\}$	$\{u_{i_o}^o\}$

The type I laws are derived by applying the theory of linear gaussian systems having quadratic performance indices. The control sequences associated with the type II laws are derived by including an explicit constraint on control level in the guidance problem formulation.

4.2 CONCLUSIONS

The important conclusions deduced from computer simulation results about the various guidance laws are summarized below:

- When the acceleration limiter is active -- i.e., when $\{u_{i_o}^o\}$ and $\{u_{i_{oo}}\}$ differ significantly from $\{u_1^o\}$ and $\{u_{i_o}\}$ respectively -- the type II guidance law, $\{u_{i_o}^o\}$ provides a substantially smaller miss distance (as much as fifty percent smaller) than the type I law, $\{u_{i_{oo}}\}$.

- The type II laws are significantly simpler to mechanize than the type I laws; the feedback gains for the former are derived analytically by solving appropriate algebraic equations, whereas the gains for the latter are determined numerically by iteratively processing the required matrix difference equations.

- The type II laws call for average control levels that are much larger than those associated with the type I laws -- typically ten times larger. Also the type II laws are bang-bang in nature, a fact that may have an adverse effect where significant body bending modes exist.

- The predictive acceleration limiter successfully provides the desired control over airframe acceleration level.

The observations that a type II guidance law ($\{u_{i_o}^o\}$) can perform significantly better and is also more easily mechanized than the corresponding type I ($\{u_{i_o}\}$) law are important developments from this research.

The above conclusions provide several criteria for selecting a guidance law for a particular application. If the lowest possible terminal

miss distance is desired, without regard for the amount of control energy expended, the type II laws are preferred. The most significant performance advantage of the latter exists in those applications where terminal guidance accuracy is significantly limited by the maximum allowable (or achievable) missile maneuvering acceleration level. If control energy consumption must be lower than that associated with the type II laws, the type I laws can be used. A third possibility which combines the best of both techniques is a dual mode procedure, using a type I law to conserve control energy far from the target and a type II law at short range to reduce terminal miss.

Some additional comments about the potential computational requirements of the guidance system are in order. Both types of laws require the same time-varying linear state estimator -- a Kalman filter. For the planar motion problem considered in this report, a five-state filter was employed to estimate the state variables associated with the target, the missile translational motion relative to the target, and the autopilot. In an actual application it is likely that a simpler three-state filter -- obtained by assuming that autopilot state variable measurement errors are negligible -- would yield satisfactory operation. In addition to a filter, each guidance law uses a set of time-varying feedback gains to generate the feedback commands. We have pointed out the fact that the gains for the type II laws are more easily calculated. In circumstances where the dynamics defining the guidance problem are known a priori, the feedback gains required for all guidance laws can be calculated prior to flight. Thus each gain can be approximated as a simple polynomial and stored in the guidance computer. However if some important dynamic parameters -- such as those associated with the missile airframe -- are unknown and must be identified on-line, then the system gains must be

calculated on-line. In the latter situation, the computational advantage of the nonlinear-type laws is quite significant.

It is likely that a number of simplifications to the above guidance laws could be made without seriously degrading performance. For example, less frequent updating of filter and feedback gains can be tried; in some cases constant gains may be adequate. It may also be desirable to predesign the missile autopilot (making it adaptive if necessary) and then neglect autopilot dynamics in formulating the guidance problem; this is found to be a reasonable procedure in the simpler applications treated in Ref. 6. The investigation of such modifications is a logical extension of the work reported here.

4.3 TOPICS FOR FUTURE RESEARCH

The investigation described here includes many effects that are actually encountered in a tactical missile engagement -- measurement noise, target maneuvers, bounded controls, bounded acceleration, airframe dynamics, etc. The study indicates that guidance laws which are derived taking into account bounded missile control level can offer significant performance advantages when realistic levels of measurement noise and target acceleration exist. However a more complete evaluation of the guidance laws is needed, including the following tasks:

- Analysis of the sensitivity of the stochastic guidance laws described above to errors in modeling sensor noise, target motion, and missile autopilot dynamics should be performed. The objective is to determine which guidance law is least affected by imperfect knowledge of the guidance equations of motion.

- A detailed comparative evaluation of various guidance laws -- including, classical methods such as proportional guidance, pursuit guidance, etc. operating in the presence of homing sensor noise, a maneuvering target, and control surface limiting -- should be carried out to provide performance curves that are useful for system specification.

The outcome of such a study would be indications of the ultimate performance that can be achieved in a given tactical situation with a given missile design.

Another topic of interest is the derivation of guidance laws which account for intelligent target maneuvers. This is motivated by the possibility that the enemy target may know what type of guidance law is being used against him; therefore he may be able to employ a rational evasion technique that will achieve larger miss distances than if he used random maneuvers. Investigation of this problem through the use of differential game theory is recommended.

APPENDIX A

OPTIMAL STOCHASTIC CONTROL OF LINEAR SYSTEMS

The subject of optimal stochastic control is concerned with determining control policies which optimize some probabilistic measure of performance for stochastic dynamical systems. The techniques studied in this report apply only to systems with equations of motion that are linear in both the state and the open loop control variables* and with observations that are also linear combinations of the state variables. For this special case the theory of stochastic control is fairly complete for both continuous and discrete time systems and has been extensively documented. This appendix summarizes the main results for discrete time systems with appropriate references to the literature, omitting those mathematical proofs that are readily available elsewhere.

It should also be mentioned that a large body of theory exists for stochastic control systems having nonlinear equations of motion, especially for discrete systems (e.g., Refs. 9 and 10). However, few results are available that lead to practical control laws.

A.1 PROBLEM FORMULATION

A linear continuous stochastic dynamic system is defined by differential equations of the form

$$\dot{\underline{x}}(t) = F(t)\,\underline{x}(t) + G(t)\,\underline{u}(t) + \underline{w}(t) \qquad \text{(A.1-1)}$$

*That is, Eq. (A.1-1) is linear in $\underline{x}(t)$ and $\underline{u}(t)$, regardless of how $\underline{u}(t)$ may be generated. For example, $\underline{u}(t)$ may be a nonlinear function of $\underline{x}(t)$.

where F(t) and G(t) are known time-varying matrices, $\underline{x}(t)$ is the n-dimensional state vector, u(t) is an m-dimensional set of control variables, and $\underline{w}(t)$ is an n-dimensional random disturbance input to the system. It is usually assumed that $\underline{w}(t)$ is a Gaussian random process, also called "process noise," having the following statistical characteristics:*

$$\text{Mean Value: } E\left\{\underline{w}(t)\right\} = \underline{0}$$

$$\text{Covariance Matrix: } E\left\{\underline{w}(t)\,\underline{w}(\tau)^T\right\} = Q(t)\,\delta(t-\tau) \qquad \text{(A.1-2)}$$

The quantity $\delta(t-\tau)$ is the unit impulse (Dirac delta) function and Q(t) is a known positive semidefinite matrix. Although Eq. (A.1-2) specifies that $\underline{w}(t)$ has zero mean, a nonzero mean can readily be included when it is known.

To complete the specification of the system dynamics described by Eq. (A.1-1), the initial state must be provided. We assume that $\underline{x}(t_0)$ is a vector gaussian random variable having known mean and covariance matrix given by

$$E\left\{\underline{x}(t_0)\right\} \triangleq \underline{\mu}$$

$$E\left\{\left[\underline{x}(t_0) - \underline{\mu}\right]\left[\underline{x}(t_0 - \underline{\mu}\right]^T\right\} \triangleq P_0 \qquad \text{(A.1-3)}$$

The above model defines $\underline{w}(t)$ as a "white noise" random process which has the property that sample values taken at different time instants are uncorrelated. If the latter condition does not hold for the system under investigation, Eq. (A.1-1) can often be modified to obtain a valid

*E { } denotes mathematical expectation.

mathematical model that does have white process noise.* The assumption that the process noise is gaussian is often physically reasonable because many random disturbances can be accurately modeled as a superposition of a large number of statistically independent random events. The resulting aggregate process has a probability distribution that approaches the gaussian distribution as the number of constituent events becomes large, regardless of the probability distributions of the individual events.** In addition, gaussian processes have the desirable mathematical property that their gaussian character is preserved when they are "passed through" a linear system, such as the one represented by Eq. (A.1-1). That is, if $\underline{w}(t)$ and $\underline{x}(t_0)$ are gaussian and $\underline{u}(t)$ is a known function of time on an interval $t_0 \leq t \leq t_1$, then $\underline{x}(t_1)$ is also gaussian; the mean value of $\underline{x}(t_1)$ is determined by the initial mean, $\underline{\mu}$, and the known history of $\underline{u}(t)$.

In order that a feedback control policy can be mechanized, measurements related to the state vector $\underline{x}(t)$ must be available. In a physical system such measurements are typically obtained by sensors whose outputs are observations of known functions of the state variables corrupted by measurement errors. Furthermore, measurements frequently can be observed or accepted only at discrete time instants, $t_i (i = 0, 1, \ldots)$, either because the sensor inherently operates as a sampler or because a digital computer is used to process the measurement data. For missile applications the above conditions can usually be expressed by the linear measurement equation,

$$\underline{z}_i = H_i \underline{x}_i + \underline{v}_i; \qquad i = 0, 1, \ldots \qquad \text{(A.1-4)}$$

*For example, the time-correlated process can often be regarded as the output of a linear system driven by white noise and the state variables associated with the latter are included in the definition of $\underline{x}(t)$.

**This is a paraphrase of the "central limit theorem" (see Ref. 11).

In Eq. (A.1-4), $\underline{z}_i$ is a q-dimensional measurement vector, H_i is a known matrix and $\{\underline{v}_i\}$ is a gaussian white noise* sequence specified by

$$E\left\{\underline{v}_i\right\} = \underline{0} \qquad \text{for all } i$$

$$E\left\{\underline{v}_i \underline{v}_j^T\right\} = \begin{cases} R_i; & i = j \\ 0; & i \neq j \end{cases} \qquad \text{(A.1-5)}$$

where R_i is a positive definite matrix. The noise sequence accounts for the measurement errors and H_i accommodates all situations where the measurements are linear functions of the state variables. The noise covariance matrix R_i is assumed to be positive definite. It is also usually reasonable to assume that the process $\underline{w}(t)$ is uncorrelated with the sequence $\{\underline{v}_i\}$; however the subsequent discussion can easily be modified if this condition does not hold (see Ref. 12).

An optimal feedback control law is to be selected for $\underline{u}(t)$ in Eq. (A.1-1) so that an appropriate performance index J is minimized. We will allow $\underline{u}(t)$ to be a function of all measurements that have been taken up to time t. Just as in the case of the measurements, it is usually true that new values of the control can be computed only at discrete instants of time because of the data processing requirements. Consequently we assume here that $\underline{u}(t)$ is to be held constant at the value $\underline{u}_i$ over the interval $t_i \leq t < t_{i+1}$ where t_i is coincident with the measurement time**; therefore

*For the case where the measurement noise is known to be correlated in time see Ref. 12.

**In some situations it may be possible to process measurements faster than control changes can be computed; in other cases some measurements e.g., a gyro output) may be obtainable more frequently than others e.g., a homing sensor output). These possibilities can readily be included in the theory; however, for convenience of exposition, the measurement and control computation times are considered to be identical here.

the problem of obtaining $\underline{u}(t)$ reduces to that of determining the sequence $\{\underline{u}_i\}$ The latter consideration motivates the following choice for the form of the performance index.*

$$J = \underset{\{\underline{x}_i\}}{E} \left\{ f\left(\underline{x}(t_N), t_N\right) + \sum_{i=0}^{N-1} L_i\left(\underline{x}(t_i), \underline{u}_i, t_i\right) \right\} \qquad \text{(A.1-6)}$$

where t_0 and t_N are specified initial and final times. In addition there may be a constraint on $\{\underline{u}_i\}$ of the form**

$$\underline{u}_i \in \Omega_i \qquad \text{(A.1-7)}$$

where Ω_i is a specified region in m-dimensional euclidean space. For example, if we require $|\underline{u}_i| \leq 1$ for all i, then Ω_i is an m-dimensional box with sides two units long. The expectation operation is required in Eq. (A.1-6) because the index can be minimized only in a statistical sense; the actual value of the quantity inside the brackets cannot be evaluated because $\underline{x}(t)$ is a random process.

Because the performance index depends upon the state and control variables at discrete instants of time, differential equations (Eqs. (A.1-1)) are not required to describe the dynamic behavior of the system. Instead, difference equations -- derived from the differential equations -- which relate the value of the state at time t_i to its value at time t_{i+1} are sufficient. The latter are readily obtained from Eqs. (A.1-1) and (A.1-2)

---

*The notation $\underset{\{\underline{x}_i\}}{E}\ \{\ \}$ means that the mathematical expectation is to be carried out over all the random variables, $\underline{x}(t_i)$ -- i = 0, 1, ..., N -- appearing within the braces.

**The symbol $\in$ means "is contained in."

using the properties of the solutions of linear stochastic differential equations (see Ref. 12 or 13); these expressions together with the other relations needed for the optimization problem are summarized below:

Discrete Time Optimal Stochastic Control Problem — Determine the optimal piecewise constant feedback control policy as a function of all past measurements,*

$$u(t) = \underline{u}_i^o\left(\underline{Z}_j, t_i\right); \qquad t_i \le t \le t_{i+1}$$
$$Z_i \triangleq \{\underline{z}_j\} \qquad ; \qquad 0 \le j \le i \tag{A.1-8}$$

which minimizes the performance index

$$J = \underset{\{\underline{x}_i\}}{E}\left\{f\left(\underline{x}_N, t_N\right) + \sum_{i=0}^{N-1} L_i\left(\underline{x}_i, \underline{u}_i, t_i\right)\right\} \tag{A.1-9}$$

for a specified value of t_N, subject to the discrete time constraint equations

$$\underline{x}_{i+1} = \Phi_i \underline{x}_i + \Gamma_i \underline{u}_i + \underline{w}_i$$
$$\underline{z}_i = H_i \underline{x}_i + \underline{v}_i$$
$$\underline{u}_i \in \Omega_i$$
$$E\left\{\underline{x}_0\right\} = \underline{\mu}\,; \qquad E\left\{\left(\underline{x}_0 - \underline{\mu}\right)\left(\underline{x}_0 - \underline{\mu}\right)^T\right\} = P_0 \tag{A.1-10}$$

The matrices Φ_i and Γ_i in Eq. (A.1-10) are related to the parameters in Eqs. (A.1-1) and (A.1-2) by

*The superscript "o" denotes an optimal control. The symbol Z_i denotes the sequence of all measurements observed up through time t_i.

$$\Phi_i \triangleq \Phi\left(t_{i+1}, t_i\right)$$

$$\dot{\Phi}\left(t, t_i\right) = F(t)\,\Phi\left(t, t_i\right); \qquad \Phi\left(t_i, t_i\right) = I \tag{A.1-11}$$

$$\Gamma_i \triangleq \int_{t_i}^{t_{i+1}} \Phi\left(t_{i+1}, \tau\right) G(\tau)\, d\tau \tag{A.1-12}$$

The sequences $\{\underline{w}_i\}$ and $\{\underline{v}_i\}$ are gaussian white noise sequences satisfying the conditions,

$$E\left\{\underline{w}_i\right\} = E\left\{\underline{v}_i\right\} = \underline{0}$$

$$E\left\{\underline{w}_i \underline{w}_j^T\right\} = \begin{cases} Q_i \triangleq \int_{t_i}^{t_{i+1}} \Phi\left(t_{i+1}, \tau\right) Q(\tau)\, \Phi\left(t_{i+1}, \tau\right)^T d\tau\,; & i = j \\ 0\,; & i \neq j \end{cases}$$

$$E\left\{\underline{v}_i \underline{v}_j^T\right\} = \begin{cases} R_i\,; & i = j \\ 0\,; & i \neq j \end{cases} \tag{A.1-13}$$

The above discrete time formulation is used throughout this report. An analogous development for continuous systems is available in the cited references.

A.2 QUADRATIC PERFORMANCE INDICES AND UNCONSTRAINED CONTROL VARIABLES

A particularly important case of the discrete time optimal control problem formulated in the preceding section occurs when the performance index in Eq. (A.1-9) is a quadratic function of the state and control; i.e.,

$$J = \underset{\{\underline{x}_i\}}{E} \left\{ \underline{x}_N^T V_N \underline{x}_N + \sum_{i=0}^{N-1} \left[\underline{x}_i^T V_i \underline{x}_i + \underline{u}_i^T W_i \underline{u}_i \right] \right\} \quad (A.2\text{-}1)$$

where V_i -- i = 0,1,...,N -- are positive semidefinite matrices and W_i -- i = 0,1,...,N-1 -- are positive definite matrices. In addition, we assume the control variables are unconstrained; i.e., Ω_i in Eq. (A.1-10) is the entire m-dimensional euclidean space. This type of performance index is often chosen when the objective is to reduce the magnitude of the state without using excessive amounts of control. It tends to limit energy expenditure and it also tends to limit the magnitude of the required control level, although it does not explicitly bound the latter. Perhaps a more important reason for its popularity is that the optimal feedback control is linear and readily computed,* as demonstrated below.

Because the dynamics and measurements in Eq. (A.1-10) are linear, the optimal control sequence $\{u_i^o\}$ that minimizes J can be determined analytically (Ref. 12) in the form:

*This is a relative judgement; it is readily computed compared with solutions to many more general control problems.

$$\underline{u}_i^o = -C_i \hat{\underline{x}}_i$$

$$\hat{\underline{x}}_i = \tilde{\underline{x}}_i + K_i \left(\underline{z}_i - H_i \tilde{\underline{x}}_i \right)$$

$$\tilde{\underline{x}}_{i+1} = \Phi_i \hat{\underline{x}}_i + \Gamma_i \underline{u}_i^o \; ; \quad \tilde{\underline{x}}_0 = \underline{\mu} \qquad \text{(A.2-2)}$$

where

$$C_i = \left(\Gamma_i^T S_{i+1} \Gamma_i + W_i \right)^{-1} \Gamma_i^T S_{i+1} \Phi_i$$

$$S_i = \Phi_i^T S_{i+1} \Phi_i - C_i^T \left(W_i + \Gamma_i^T S_{i+1} \Gamma_i \right) C_i + V_i$$

$$S_N = V_N \qquad \text{(A.2-3)}$$

and

$$K_i = \tilde{P}_i H_i^T \left(H_i \tilde{P}_i H_i^T + R_i \right)^{-1}$$

$$\tilde{P}_i = \Phi_i P_i \Phi_i^T + Q_i \; ; \quad \tilde{P}_0 = P_0$$

$$P_i = \tilde{P}_i - K_i \left(H_i \tilde{P}_i H_i^T + R_i \right) K_i^T \qquad \text{(A.2-4)}$$

The associated minimum value of the performance index in Eq. (A.2-1), J; is given by*

$$J^o = \mathrm{Tr} \left\{ S_0 \left(P_0 + \underline{\mu} \underline{\mu}^T \right) + \sum_{i=0}^{N-1} S_{i+1} \left(Q_i + \Gamma_i C_i P_i \Phi_i^T \right) \right\} \qquad \text{(A.2-5)}$$

*The notation Tr { } denotes the trace of the matrix (sum of its diagonal elements) within the braces.

The quantity $\hat{\underline{x}}_i$ in Eq. (A.2-2) is the conditional mean of the gaussian vector $\underline{x}_i$, given knowledge of the control and measurement histories up through time t_i*. The conditional mean has the property that it is the best possible estimate of $\underline{x}_i$ under a wide variety of estimation criteria.** Equations (A.2-2) and (A.2-4) constitute a discrete Kalman filter which recursively calculates $\hat{\underline{x}}_i$ in terms of the known controls $\{\underline{u}_i^o\}$, the system dynamics, the random process statistics, and the measurements. The matrix K_i is referred to as the Kalman gain.

The gain matrix C_i determined from Eq. (A.2-3) is identical to that associated with the optimal control law that minimizes the deterministic performance index.

$$\underline{x}_N^T T_N \underline{x}_N + \sum_{i=0}^{N-1} \left(\underline{x}_i^T V_i \underline{x}_i + \underline{u}_i^T W_i \underline{u}_i \right)$$

assuming the process and measurement noise sequences in Eq. (A.1-10) are absent. Consequently the optimal stochastic controller is mechanized by two distinct operations -- an optimal linear estimator (Kalman filter) that is independent of the performance index weighting matrices, and an optimal feedback control law whose gains (Eq. (A.2-3)) are independent of the random process statistics. This is the so-called separation property for linear systems with quadratic performance indices and unconstrained controls; the structure of the controller is illustrated in Fig. A.2-1.

---

* The conditional mean includes the effect on the state in Eq. (A.1-10) of a known control input as well as the unknown initial conditions and the unknown process noise.

** For example, $\hat{\underline{x}}_i$ is the value of $\bar{\underline{x}}_i$ which minimizes

$$E\left\{ \left(\underline{x}_i - \bar{\underline{x}}_i \right)^T \Lambda \left(\underline{x}_i - \bar{\underline{x}}_i \right) \right\}$$

where Λ is any positive semidefinite matrix.

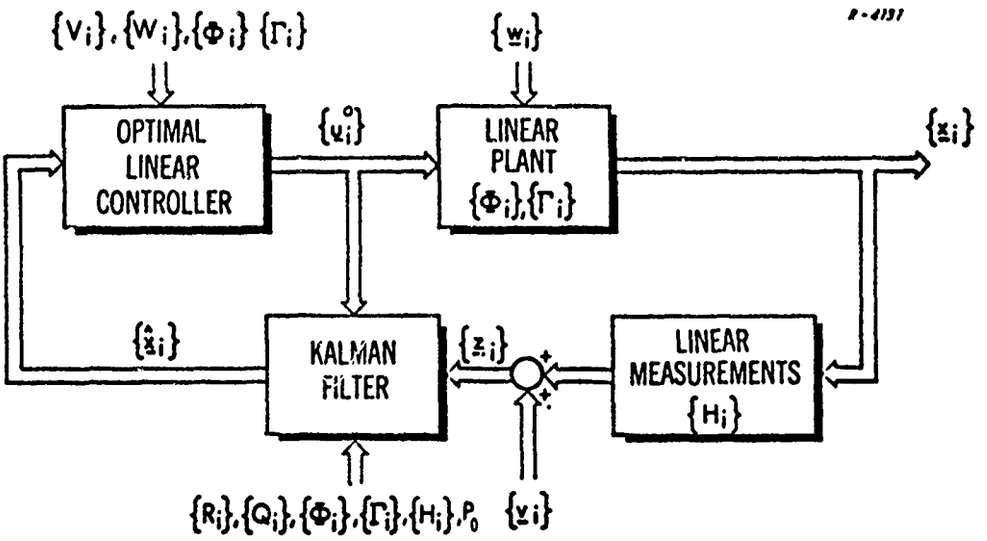

Figure A.2-1 Structure of the Optimal Stochastic Controller for a Linear Plant with a Quadratic Performance Index

The linear control law described above is relatively simple to implement. When the parameters defining the matrices Φ_i, Γ_i, etc. in Eqs. (A.2-2) through (A.2-4) are known apriori,* the gains C_i and K_i can be precomputed and stored in a computer so that the only on-line calculations required are those specified in Eq. (A.2-2). However, the assumptions of a quadratic performance index and an unconstrained control level are unrealistic for some problems. In the next section more general design criteria are considered.

*The parameters of a tactical missile guidance problem are not always known apriori; this point is discussed in Section 2.1.

**Often simple polynomial approximations to the gain histories are adequate.

A.3 GENERAL PERFORMANCE INDICES AND CONSTRAINED CONTROL VARIABLES

This section outlines the method of solving the discrete optimal control problem posed in Section A.2 for a linear system with the performance index

$$J = \underset{\{\underline{x}_i\}}{E}\left\{f\left(\underline{x}_N, t_N\right) + \sum_{i=0}^{N-1} L_i\left(\underline{x}_i, \underline{u}_i, t_i\right)\right\} \qquad \text{(A.3-1)}$$

The derivation presented here uses a dynamic programming approach, as in Ref. 14. We first assume time t_N has occurred and the complete optimal control sequence $\{\underline{u}_i^o\}$ has been applied using the observed measurements $\{\underline{z}_i\}$. Then proceeding backward from stage to stage, we determine the individual commands $\underline{u}_{N-1}^o$, $\underline{u}_{N-2}^o$, ... needed to minimize the "cost to complete the process" J_{N-1}, J_{N-2}, ... defined by

$$J_{N-j} \triangleq \underset{\substack{\{x_i\} \\ N-j \le i \le N-1}}{E}\left\{f\left(\underline{x}_N, t_N\right) + \sum_{i=N-j}^{N-1} L_i\left(\underline{x}_i, \underline{u}_i, t_i\right)\right\}$$

In this way we can derive a recursive expression from which each optimal control command can be derived in terms of the control commands and measurements that preceded it in time, providing a feedback control law. In the general case this recursive relation is difficult to solve, requiring extensive numerical calculation; however we shall see that the guidance problem posed in Chapter 2 can be solved analytically. To aid the discussion it is convenient to use the notation

$$U_k^o \triangleq \left\{\underline{u}_i^o\right\} \quad ; \quad 0 \le i \le k$$

$$Z_k \triangleq \left\{\underline{z}_i\right\} \quad ; \quad 0 \le i \le k$$

That is, U_k^o and Z_k denote the sequences of all optimal controls that have been applied and all measurements that have been observed up through time t_k.

To begin, we assume that all stages of the process have been completed and we are at time t_N. There are no more optimal controls to be computed and the optimal value of the terminal cost, J_N^o, is defined by

$$J_N^o \triangleq \underset{\underline{x}_N}{E} \left\{ f(\underline{x}_N) \,\middle|\, U_{N-1}^o, Z_N \right\} \qquad \text{(A.3-2)}$$

which is shorthand notation for the expectation operation

$$J_N^o = \int \cdots \int f(\underline{x}_N)\, p(\underline{x}_N \,|\, U_{N-1}^o, Z_N)\, d\underline{x}_N \qquad \text{(A.3-3)}$$

The quantity $p(\underline{x}_N | U_{N-1}^o, Z_N)$ is the conditional probability density function* of $\underline{x}_N$, as determined by the known measurement and control sequences, and $d\underline{x}_N$ denotes the n-dimensional "volume" element $dx_1(t_N)\, dx_2(t_N) \ldots dx_n(t_N)$. The limits of integration on each integral in Eq. (A.3-3) are from minus infinity to plus infinity; for convenience, they are omitted from the notation throughout this discussion, always being understood as infinite. Now at time t_N, $\underline{x}_N$ is a random variable whose mean value is a function of the control history, the observed measurement history, the statistics of the initial state $\underline{x}_0$ in Eq. (A.1-3), and the statistics

*Throughout this report, a function of the form $p(\underline{x}|\underline{y})$ denotes the conditional probability density of $\underline{x}$, depending upon a known value of $\underline{y}$. This is an abuse of conventional notation which uses the symbol, $p_{\underline{x}|\underline{y}}(\underline{\xi}|\underline{\eta})$, where $\underline{\xi}$ and $\underline{\eta}$ denote particular values of $\underline{x}$ and $\underline{y}$, respectively. The shortened notation used here should be clear to the reader, keeping in mind the fact that $p(\underline{y}|\underline{x})$ and $p(\underline{x}|\underline{y})$ are two different functions of the same variables, $\underline{x}$ and $\underline{y}$; that is, $p(\underline{y}|\underline{x}) \neq p(\underline{x}|\underline{y})\Big|_{\underline{y} \to \underline{x},\, \underline{x} \to \underline{y}}$.

of the measurement and process noise sequences.* In addition the following important conditions are satisfied at time t_N:

- The random sequences $\{\underline{w}_i\}$ and $\{\underline{v}_i\}$ in Eq. (A.1-10) are gaussian.
- The control and measurement histories, U_{N-1}^o and Z_N, are known.
- Both the process dynamics and the measurements (Eq. (A.1-10)) are linear functions of the state.

Therefore, $\underline{x}_N$ is "conditionally gaussian;" i.e., $p(\underline{x}_N | U_{N-1}, Z_N)$ is a gaussian function that is completely specified by the conditional mean $\hat{\underline{x}}_N$ and covariance matrix P_N of $\underline{x}_N$, defined by

$$\hat{\underline{x}}_N \triangleq \int \cdots \int \underline{x}_N \, p\left(\underline{x}_N \middle| U_{N-1}^o, Z_N\right) d\underline{x}_N$$

$$P_N \triangleq \int \cdots \int \left(\underline{x}_N - \hat{\underline{x}}_N\right)\left(\underline{x}_N - \hat{\underline{x}}_N\right)^T p\left(\underline{x}_N \middle| U_{N-1}^o, Z_N\right) d\underline{x}_N$$

The functional form of $p(\underline{x}_N | U_{N-1}^o, Z_N)$, expressed in terms of $\hat{\underline{x}}_N$ and P_N, is given by

$$p\left(\underline{x}_N \middle| U_{N-1}^o \, Z_N\right) = 2\pi^{-n/2} \left| P_N \right|^{-1/2} \exp\left\{-\frac{1}{2}\left(\underline{x}_N - \hat{\underline{x}}_N\right)^T P_N^{-1} \left(\underline{x}_N - \hat{\underline{x}}_N\right)\right\}$$

*As in Section A.2, the mean of the state at any time t contains a component produced by the known control sequence applied up through time t as well as a component derived from previously observed measurement data.

Now because of the three conditions listed immediately above, $\hat{\underline{x}}_N$ can be determined by a Kalman filter acting on the measurement data Z_N and known controls U^o_{N-1} as specified by Eqs. (A.2-2) and (A.2-4); furthermore, P_N is a deterministic quantity (i.e., it is independent of the measurements) provided by Eq. (A.2-4) at stage i = N. Therefore, substituting the above expression for $p(\underline{x}_N | U^o_{N-1}, Z_N)$ into Eq. (A.3-3), J^o_N can be calculated as a function of $\hat{\underline{x}}_N$;

$$J^o_N = \bar{f}\left(\hat{\underline{x}}_N\right) \qquad \text{(A.3-4)}$$

The over-bar notation refers to the averaging operation performed in Eq. (A.3-3). The significant property of Eq. (A.3-4) is that the dependence of J^o_N on all random variables can be expressed solely in terms of $\hat{\underline{x}}_N$ and a number of deterministic quantities such as covariance matrices, plant dynamics, etc. The latter are suppressed in the notation.

Next suppose that all but the last step of the process defined by Eq. (A.1-10) has been completed using the collections of known optimal controls and measurements, U^o_{N-2} and Z_{N-1}. Therefore referring to Eq. (A.3-1), at time t_{N-1} we need to determine the value of $\underline{u}_{N-1}, \underline{u}^o_{N-1}$, which minimizes the cost to complete the process,

$$J_{N-1} = \underset{\underline{x}_{N-1}, \underline{x}_N}{E} \left\{ f\left(\underline{x}_N\right) + L_{N-1}\left(\underline{x}_{N-1}, \underline{u}_{N-1}, t_{N-1}\right) \right\}$$

This minimization is indicated by defining the optimal cost to complete the process by*

*The notation $\min_{\underline{\alpha} \in A} \{\ \}$ means that the value of $\underline{\alpha}$ within the set A is to be determined which minimizes the quantity inside the braces.

$$J^{o}_{N-1} = \min_{\underline{u}_{N-1} \in \Omega_{N-1}} \left\{ E_{\underline{x}_{N-1}, \underline{x}_N} \left\{ \left[f\left(\underline{x}_N\right) + \left(L_{N-1}, \underline{x}_{N-1}, \underline{u}_{N-1}, t_{N-1}\right) \right] \middle| U^{o}_{N-2}, Z_{N-1} \right\} \right\} \tag{A.3-5}$$

where the notation -- $| U^{o}_{N-2}, Z_{N-1}$ -- emphasizes that the known controls and measurements are used to define the conditional probability density functions for $\underline{x}_{N-1}$ and $\underline{x}_N$.

Equation (A.3-5) can be investigated in two parts. By applying the same argument used for Eq. (A.3-2) and assuming for the moment that the minimization over $\underline{u}_{N-1}$ has been carried out so that $\underline{u}_{N-1} = \underline{u}^{o}_{N-1}$ is known, the first expectation in Eq. (A.3-5) can be written as

$$\bar{L}\left(\hat{\underline{x}}_{N-1}, \underline{u}^{o}_{N-1}, t_{N-1}\right) \triangleq E_{\underline{x}_{N-1}} \left\{ L_{N-1}\left(\underline{x}_{N-1}, \underline{u}^{o}_{N-1}, t_{N-1}\right) \middle| U^{o}_{N-2}, Z_{N-1} \right\} \tag{A.3-6}$$

because L_{N-1} is independent of $\underline{x}_N$. Just as we found at the N^{th} measurement time, $\underline{x}_{N-1}$ is a gaussian random variable and its conditional mean $\hat{\underline{x}}_{N-1}$ is provided by a Kalman filter operating on the measurement history Z_{N-1} and the control history U^{o}_{N-2} (note that $\hat{\underline{x}}_{N-1}$ is independent of $\underline{u}^{o}_{N-1}$). Continuing with our assumption that $\underline{u}^{o}_{N-1}$ is known, the second expectation in Eq. (A.3-5) can be expressed as follows:

$$\tilde{J}_N \triangleq E_{\underline{x}_N} \left\{ f\left(\underline{x}_N\right) \middle| U^{o}_{N-2}, Z_{N-1} \right\} = E_{\underline{x}_N} \left\{ f\left(\underline{x}_N\left(\underline{u}^{o}_{N-1}\right)\right) \middle| U^{o}_{N-2}, Z_{N-1} \right\}$$

$$= E_{\underline{x}_N} \left\{ f\left(\underline{x}_N\right) \middle| U^{o}_{N-2}, \underline{u}^{o}_{N-1}, Z_{N-1} \right\} \tag{A.3-7}$$

The sequence of equalities in Eq. (A.3-7)* holds because $\underline{x}_N$ can be regarded as a function of the control $\underline{u}^o_{N-1}$ (assumed known as a function of Z_{N-1}); therefore each term is an equivalent expression for the expectation conditioned on U^o_{N-2}, $\underline{u}^o_{N-1}$, and Z_{N-1}. Now compare Eq. (A.3-5) with Eqs. (A.3-6) and (A.3-7), where we have assumed throughout that $\underline{u}^o_{N-1}$ is known, and observe that

$$J^o_{N-1} = \bar{L}\left(\hat{\underline{x}}_{N-1},\ \underline{u}^o_{N-1}, t_{N-1}\right) + \tilde{J}_N \qquad \text{(A.3-8)}$$

Using the identity

$$p(\underline{x}\,|\,\underline{y}) = \int\cdots\int p(\underline{x}|\underline{y},\underline{z})\, p(\underline{z}\,|\,\underline{y})\, d\underline{z} \triangleq \underset{\underline{z}}{E}\left\{p(\underline{x}|\underline{y},\underline{z})\,|\,\underline{y}\right\} \qquad \text{(A.3-9)}$$

for probability density functions of the random vectors $\underline{x}$ and $\underline{z}$, given a known value of $\underline{y}$, Eq. (A.3-7) can be expanded as follows

$$\begin{aligned}
\tilde{J}_N &= \underset{\underline{x}_N}{E}\left\{f(\underline{x}_N)\,\middle|\,U^o_{N-2},\ \underline{u}^o_{N-1},\ Z_{N-1}\right\} \\
&= \int\cdots\int f(\underline{x}_N)\,\underset{\underline{z}_N}{E}\left\{p\left(\underline{x}_N\middle|\,U^o_{N-2},\underline{u}^o_{N-1},Z_N\right)\middle|\,U^o_{N-2},\underline{u}^o_{N-1},Z_{N-1}\right\} d\underline{x}_N \\
&= \underset{\underline{z}_N}{E}\left\{\underset{\underline{x}_N}{E}\left\{f(\underline{x}_N)\,\middle|\,U^o_{N-2},\underline{u}^o_{N-1},\ Z_N\right\}\middle|\,U^o_{N-2},\ \underline{u}^o_{N-1},\ Z_{N-1}\right\}
\end{aligned} \qquad \text{(A.3-10)}$$

*Compare Eq. (A.3-7) with Eq. (A.3-3) and note that $\tilde{J}_N$ is different from J^o_N because $\tilde{J}_N$ is conditioned on the measurements only up to time t_{N-1} whereas J^o_N is conditioned on the measurements up to time t_N.

A comparison of the last line of Eq. (A.3-7) with Eqs. (A.3-2) and (A.3-4) reveals that

$$\tilde{J}_N = \underset{\underline{z}_N}{E}\left\{J_N^o\left(\hat{\underline{x}}_N\right)\middle| U_{N-2}^o, \underline{u}_{N-1}^o, Z_{N-1}\right\} \qquad \text{(A.3-11)}$$

Substitution of Eq. (A.3-11) into (A.3-8) produces

$$J_{N-1}^o = \bar{L}_{N-1}\left(\hat{\underline{x}}_{N-1}, \underline{u}_{N-1}^o, t_{N-1}\right) + \underset{\underline{z}_N}{E}\left\{J_N^o\left(\hat{\underline{x}}_N\right)\middle| U_{N-2}^o, \underline{u}_{N-1}^o, Z_{N-1}\right\} \qquad \text{(A.3-12)}$$

Now recall our assumption that the optimal control $\underline{u}_{N-1}^o$ at stage N-1 is known; however, in fact our objective is to determine it from the functional form of J_{N-1}^o. This is accomplished by rewriting Eq. (A.3-12) in the equivalent form

$$J_{N-1}^o = \min_{\underline{u}_{N-1} \in \Omega_{N-1}}\left\{\bar{L}_{N-1}\left(\hat{\underline{x}}_{N-1}, \underline{u}_{N-1}, t_{N-1}\right) + \underset{\underline{z}_N}{E}\left\{J_N^o\left(\hat{\underline{x}}_N\right)\middle| U_{N-2}^o, \underline{u}_{N-1}, Z_{N-1}\right\}\right\} \qquad \text{(A.3-13)}$$

and by carrying out the indicated minimization over $\underline{u}_{N-1}$. Equation (A.3-13) has the important property that the optimal cost to complete the process at stage N-1 can be expressed in terms of the "incremental cost" $\bar{L}_{N-1}$ and the optimal terminal cost J_N^o which we computed at stage N (see Eqs. (A.3-2) through (A.3-4)). This has the recursive form which we desire; now we proceed to show that the dependence of $\underline{u}_{N-1}^o$ upon previous controls and measurements can be expressed solely in terms of $\hat{\underline{x}}_{N-1}$.

In order to determine $\underline{u}_{N-1}^o$ we must be able to compute the averages defined in Eq. (A.3-13). This can be done using the properties

of Eqs. (A.3-6) and (A.3-11). From Eq. (A.3-6) we have

$$\bar{L}\left(\hat{\underline{x}}_{N-1}, \underline{u}_{N-1}, t_{N-1}\right) = \int \cdots \int L_{N-1}\left(\underline{x}_{N-1}, \underline{u}_{N-1}, t_{N-1}\right) p\left(\underline{x}_{N-1} \middle| U^{o}_{N-2}, Z_{N-1}\right) d\underline{x}_{N-1}$$

$$= \frac{\int \cdots \int L_{N-1}\left(\underline{x}_{N-1}, \underline{u}_{N-1}, t_{N-1}\right) \exp\left\{-\frac{1}{2}\left(\underline{x}_{N-1} - \hat{\underline{x}}_{N-1}\right)^{T} P^{-1}_{N-1}\left(\underline{x}_{N-1} - \hat{\underline{x}}_{N-1}\right)\right\} d\underline{x}_{N-1}}{(2\pi)^{n/2}\sqrt{\text{Det}\left(P_{N-1}\right)}}$$

(A.3-14)

where $\hat{\underline{x}}_{N-1}$ and $\underline{P}_{N-1}$ are provided by the Kalman filter equations -- Eqs. (A.2-2) and (A.2-4) -- operating on the measurement and control histories, Z_{N-1} and U^{o}_{N-2}. To compute the second expectation in Eq. (A.3-13), recall from Eq. (A.2-2) that the Kalman filter output at stage N is given by

$$\hat{\underline{x}}_{N} = \Phi_{N-1}\hat{\underline{x}}_{N-1} + \Gamma_{N-1}\underline{u}_{N-1} + K_{N}\left[\underline{z}_{N} - H_{N}\left(\Phi_{N-1}\hat{\underline{x}}_{N-1} + \Gamma_{N-1}\underline{u}_{N-1}\right)\right]$$

(A.3-15)

In addition, using Eq. (A.1-10) note that the measurement $\underline{z}_{N}$ can be written as

$$\underline{z}_{N} = H_{N}\left(\Phi_{N-1}\underline{x}_{N-1} + \Gamma_{N-1}\underline{u}_{N-1} + \underline{w}_{N-1}\right) + \underline{v}_{N-1} \qquad \text{(A.3-16)}$$

Now regarding $\underline{u}_{N-1}$ as a set of parameters to be determined and knowing that $\underline{x}_{N-1}$, $\underline{w}_{N-1}$, and $\underline{v}_{N-1}$ are all independent gaussian random variables, it follows that $\underline{z}_{N}$ is a gaussian random variable whose mean and covariance can be derived directly from Eq. (A.3-16);

$$E\left\{\underline{z}_{N}\right\} \triangleq \hat{\underline{z}}_{N} = H_{N}\left(\Phi_{N-1}\hat{\underline{x}}_{N-1} + \Gamma_{N-1}\underline{u}_{N-1}\right)$$

$$E\left\{\left(\underline{z}_{N} - \hat{\underline{z}}_{N}\right)\left(\underline{z}_{N} - \hat{\underline{z}}_{N}\right)^{T}\right\} \triangleq \Sigma_{N} = H_{N}\left(\Phi_{N-1} P_{N-1} \Phi^{T}_{N-1} + Q_{N-1}\right)H^{T}_{N} + R_{N-1}$$

(A.3-17)

If we define

$$\underline{\xi}_N = \underline{z}_N - \hat{\underline{z}}_N \tag{A.3-18}$$

and substitute Eqs. (A.3-16), (A.3-17), and (A.3-18) into Eq. (A.3-15) the result is

$$\hat{\underline{x}}_N = \Phi_{N-1}\hat{\underline{x}}_{N-1} + \Gamma_{N-1}\underline{u}_{N-1} + K_N\underline{\xi}_N \tag{A.3-19}$$

where $\underline{\xi}_N$, the so-called measurement residual, is a zero mean gaussian random variable having covariance equal to Σ_N in Eq. (A.3-17). Therefore the second expectation in Eq. (A.3-13) can be written as

$$\underset{\underline{z}_N}{E}\left\{J_N^o(\hat{\underline{x}}_N) \,\middle|\, U_{N-2}^o, \underline{u}_{N-1}, Z_{N-1}\right\} = \frac{\int\cdots\int J_N^o\left(\Phi_{N-1}\hat{\underline{x}}_{N-1} + \Gamma_{N-1}\underline{u}_{N-1} + \underline{\lambda}\right)\exp\left\{-\frac{1}{2}\underline{\lambda}^T\Lambda^{-1}\lambda\right\}d\underline{\lambda}}{(2\pi)^{n/2}\sqrt{\text{Det}(\Lambda)}}$$

$$\Lambda \triangleq K_N\Sigma_N K_N^T$$

$$\underline{\lambda} \triangleq K_N\underline{\xi}_N \tag{A.3-20}$$

Equations (A.3-13), (A.3-14), (A.3-17), and (A.3-20) provide all the relations needed to calculate the optimum control $\underline{u}_{N-1}^o$ as a function of $\hat{\underline{x}}_{N-1}$ conditioned on $\underline{U}_{N-2}^o$ and Z_{N-1}. Furthermore it is clear that the dependence of J_{N-1}^o upon $\underline{U}_{N-2}^o$ and Z_{N-1} can also be expressed completely in terms of $\hat{\underline{x}}_{N-1}$, just as J_N^o depends only upon $\hat{\underline{x}}_N$ in Eq. (A.3-4). Therefore, by induction it can be established that Eqs. (A.3-13) through (A.3-20) hold if the index N is changed as follows:

$$N \rightarrow j; \qquad j = N, N-1, \ldots, 1$$

Consequently by recursively carrying out the minimization specified in Eq. (A.3-13), the entire set of optimal controls can be generated with each control $\underline{u}_i^o$ being a function of $\hat{\underline{x}}_i$. This method of solving the control problem is referred to as dynamic programming.*

Notice that a form of separation principle holds for the above optimal control law in the sense that $\underline{u}_i^o$ is always a function of the conditional mean (optimum estimate) of the state. The latter is provided by a Kalman filter in the same fashion described for quadratic performance indices in Section A.2. However, the optimal controls are not generally linear functions of the estimated state nor are they independent of the statistics of the random processes as evidenced by Eqs. (A.3-14) through (A.3-20). The mechanization of the optimal controller is illustrated in Fig. A.3-1; this should be compared with the linear system in Fig. A.2-1.

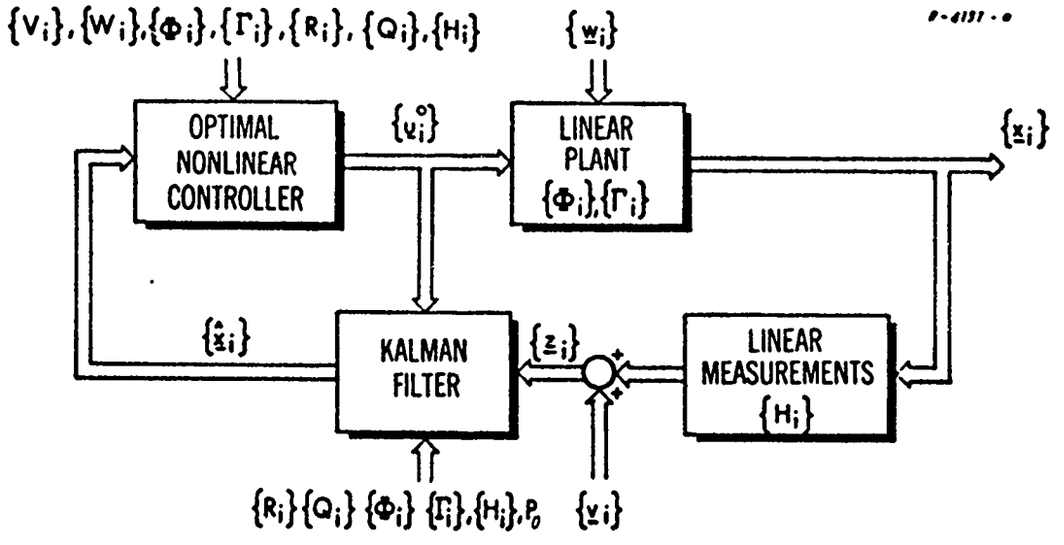

Figure A.3-1 Structure of the Optimal Stochastic Controller for a Linear Plant with a General Performance Index

*See Ref. 15 for a discussion of dynamic programming applied to stochastic control problems.

Except in special cases, the optimal controls determined from Eq. (A.3-13) cannot be determined analytically; often the dynamic programming equations must be solved numerically and the optimal control variables stored as functions of the estimated state. A great deal of computational effort and computer storage may be required to accomplish this task because of the multidimensional integrals in Eqs. (A.3-14) and (A.3-20) that must be evaluated. Some simplification can be gained by expressing these integrals as solutions to the corresponding multidimensional diffusion partial differential equation (Ref. 14). However, the amount of computation required for more than two variables of integration is still formidable. Consequently, in formulating an optimal control problem for a linear system with nonquadratic performance indices and/or constrained control variables, an effort must be made to limit the number of integrations required in Eqs. (A.3-14) and (A.3-20). Situations where this objective can be achieved are described in Section A.4.

A.4 COMPUTATIONAL CONSIDERATIONS

In the preceding section it is pointed out that there are large computational requirements associated with solving the optimal stochastic control problem for a linear system with an arbitrary performance index. To minimize the amount of computation, the dimensionality of the integrals in Eqs. (A.3-14) and (A.3-20) must be kept as low as possible. This can be accomplished by choosing a performance index that depends on as few variables as possible at each stage of the backward recursion in Eq. (A.3-13). To illustrate, suppose that $L_i = 0$ for all i in Eq. (A.2-5) and

$$J = E\left\{f(\underline{x}_N)\right\} = E\left\{f(x_1(t_N))\right\} \qquad \text{(A.4-1)}$$

where $x_1(t_N)$ denotes the first element of $\underline{x}_N$. That is, the index is a function of only one state variable at the terminal time and is independent of the state and control variables at other times. In addition, specialize Eq. (A.1-10) to the case where the control input is a scalar,

$$\underline{x}_{i+1} = \Phi_i \underline{x}_i + \underline{\gamma}_i u_i + \underline{w}_i \qquad \text{(A.4-2)}$$

and impose the constraint

$$|u_i| \leq D; \quad \text{for all } i \qquad \text{(A.4-3)}$$

where D is a specified constant. The above design criteria are realistic for the two dimensional guidance problem for a tactical missile, where $\underline{x}_1(t_N)$ corresponds to the terminal miss distance and u_i is the control surface deflection.

In order to exploit the form of Eq. (A.4-1), it is necessary to define a new state vector $\underline{y}_i$ by the linear transformation

$$\underline{y}_i \triangleq \Phi(t_N, t_i)\underline{x}_i$$

$$\Phi(t_i, t_i) = I \qquad \text{(A.4-4)}$$

The matrix $\Phi(t_N, t_i)$ is the transition matrix from time t_i to time t_N associated with Eq. (A.4-2) and determined by*

$$\Phi(t_N, t_i) = \prod_{j=N-1}^{i} \Phi_j \qquad \text{(A.4-5)}$$

*The notation $\prod_{j=n}^{m} \Phi_j$ means the product, $\Phi_n \Phi_{n-1} \cdots \Phi_{m+1} \Phi_m$

Therefore $\underline{y}_i$ is the value of the state at the terminal time produced by an initial condition $\underline{x}_i$ at time t_i with the control and process noise in Eq. (A.4-2) equal to zero. Substitution for $\underline{x}_i$ and $\underline{x}_{i+1}$ from Eq. (A.4-4) into Eq. (A.4-2) produces

$$\underline{y}_{i+1} = \underline{y}_i + \underline{\delta}_i u_i + \underline{\omega}_i$$

$$\underline{\delta}_i \triangleq \Phi\left(t_N, t_{i+1}\right)\underline{\gamma}_i \qquad \text{(A.4-6)}$$

where $\underline{\omega}_i$ is a zero-mean gaussian vector random variable with covariance matrix

$$E\left\{\underline{\omega}_i \underline{\omega}_i^T\right\} = \Phi\left(t_N, t_{i+1}\right) Q_i \Phi\left(t_N, t_{i+1}\right)^T \qquad \text{(A.4-7)}$$

and Q_i is defined in Eq. (A.1-13). Because the transformation in Eq. (A.4-4) is nonsingular,* Eq. (A.4-6) is equivalent to Eq. (A.4-2) in describing the system dynamics.

The important thing about Eq. (A.4-6) is that the first element $y_1(t_{i+1})$ of $\underline{y}_{i+1}$ is independent of the last n-1 elements of $\underline{y}_i$. Therefore, if the performance index in Eq. (A.4-1) is expressed in terms of the variables $\underline{y}_i$, the integration in Eq. (A.3-20) is performed over only one state variable. To prove this assertion it is convenient to use the fact that the optimum (Kalman filter) estimates of $\underline{x}$ and $\underline{y}$ are also related by Eq. (A.4-4) (see Ref. 13);

$$\hat{\underline{y}}_i = \Phi\left(t_N, t_i\right)\hat{\underline{x}}_i \qquad \text{(A.4-8)}$$

*The discrete time transition matrix is always nonsingular when A_i in Eq. (A.4-2) is derived by discretizing a continuous time system.

Applying Eq. (A.4-8) to Eqs. (A.3-15) through (A.3-19) it follows that

$$\hat{\underline{y}}_i = \hat{\underline{y}}_{i-1} + \underline{\delta}_{i-1}\, u_{i-1} + \Phi\left(t_N, t_i\right) \underline{\kappa}_i \underline{\xi}_i \qquad \text{(A.4-9)}$$

where $\underline{\xi}_i$ is given by Eqs. (A.3-15) and (A.3-16). The dynamics of the estimate of the first element, y_{1_i}, of $\underline{y}_i$ are therefore given by the scalar equation

$$\hat{y}_{1_i} = \hat{y}_{1_{i-1}} + \delta_{1_{i+1}}\, u_{i-1} + \alpha_i \qquad \text{(A.4-10)}$$

where α_i is a zero mean gaussian random variable and $\delta_{1_{i-1}}$ is the first element of $\underline{\delta}_{i-1}$. The mean square value of α_i is given by

$$E\left\{\alpha_i^2\right\} \triangleq \sigma_i^2 = \underline{\kappa}_1^T \Phi\left(t_N, t_i\right) K_i \Sigma_i K_i^T \Phi\left(t_N, t_i\right)^T \underline{\kappa}_1$$

$$\underline{\kappa}_1^T \triangleq [\,1\ 0\ .\ .\ 0\,] \qquad \text{(A.4-11)}$$

where Σ_i is defined by Eq. (A.3-15) with $N \to i$. Observe that the only element of $\hat{\underline{y}}_{i-1}$ appearing in Eq. (A.4-10) is $\hat{y}_{1_{i-1}}$

We also know that

$$J = E\left\{f\left(\underline{x}_N\right)\right\} = E\left\{f\left(\underline{y}_N\right)\right\} \qquad \text{(A.4-12)}$$

because $\underline{y}_N = \underline{x}_N$ according to Eq. (A.4-4). Combining Eqs. (A.4-1), (A.4-10) and (A.4-12) with Eqs. (A.3-13) and (A.3-20), letting $N \to i$ and setting $L_{i-1} = 0$ in Eq. (A.3-13) produces

$$J^{o}_{i-1}\left(\hat{y}_{1_{i-1}}\right) = \min_{\substack{u_{i-1} \\ |u_{i-1}| \le D}} \left\{ E_{\underline{z}_i} \left\{ J^{o}_{i}\left(\hat{y}_{1_i}\right) \right\} \right\} =$$

$$\min_{\substack{u_{i-1} \\ |u_{i-1}| \le D}} \left\{ \frac{1}{\sqrt{2\pi}\,\sigma_i} \int J^{o}_{i}\left(\hat{y}_{1_{i-1}} + \delta_{1_{i-1}} u_{i-1} + \alpha_i \right) \exp\left[-\frac{\alpha_i^2}{2\sigma_i^2} \right] d\alpha_i \right.$$

(A.4-13)

Thus we have reduced the problem of finding the optimal control to that of solving Eq. (A.4-13) recursively, a task that requires averaging over only one variable, α_i, as opposed to averaging over n variables, $\underline{\lambda}$, in Eq. (A.3-20).

Further simplification can be made to Eq. (A.4-13) if the index J has certain properties. In particular, suppose $J^{o}_{i}(\tau)$ is a convex,* even function** of its argument, $\tau \triangleq \hat{y}_{1_i}$, as defined by:

Even Property: $J^{o}_{i}(\tau) = J^{o}_{i}(-\tau)$

Convexity: $\frac{1}{2}\left[J^{o}_{i}(\tau_1) + J^{o}_{i}(\tau_2) \right] \ge J^{o}_{i}\left(\frac{\tau_1 + \tau_2}{2} \right)$; for all τ_1 and τ_2

(A.4-14)

Now make the definition

$$\rho \triangleq \hat{y}_{1_{i-1}} + \gamma_{1_{i-1}} u_{i-1} \qquad \text{(A.4-15)}$$

---

*The results obtained here will hold under more general assumptions; however convexity is a sufficiently broad condition for our purpose.

**Convex even functions are a very broad class; some examples are τ^2, $|\tau|$, τ^4, and $e^{|\tau|}$.

so that Eq. (A.4-13) can be rewritten as

$$J_{i-1}^{o}\left(\hat{y}_{i-1_1}\right) = \min_{\substack{u_{i-1} \\ |u_{i-1}| \le D}} \left\{\bar{J}_i^{o}(\rho)\right.$$

$$\bar{J}_i^{o}(\rho) \triangleq \frac{1}{\sqrt{2\pi}\,\sigma_i} \int J_i^{o}(\rho+\alpha) \exp\left[-\frac{\alpha^2}{2\sigma_i^2}\right] d\alpha \qquad \text{(A.4-16)}$$

If the properties in Eq. (A.4-14) hold for $J_i^{o}(\tau)$ then they also hold for $\bar{J}_i^{o}(\rho)$ with respect to the variable ρ. The even property can be demonstrated by substituting $-\rho$ for ρ in Eq. (A.4-16) and changing the variable of integration from α to λ according to

$$-\rho + \alpha = -\rho - \lambda$$

The convexity property is established by writing

$$\bar{J}_i^{o}(\rho_1) = \frac{1}{\sqrt{2\pi}\,\sigma_i} \int J_i^{o}(\rho_1+\alpha) \exp\left[-\frac{\alpha^2}{2\sigma_i^2}\right] d\alpha$$

$$\bar{J}_i^{o}(\rho_2) = \frac{1}{\sqrt{2\pi}\,\sigma_i} \int J_i^{o}(\rho_2+\alpha) \exp\left[-\frac{\alpha^2}{2\sigma_i^2}\right] d\alpha$$

$$\bar{J}_i^{o}\left(\frac{\rho_1+\rho_2}{2}\right) = \frac{1}{\sqrt{2\pi}\,\sigma_i} \int J_i^{o}\left(\frac{\rho_1+\rho_2}{2}+\alpha\right) \exp\left[-\frac{\alpha^2}{2\sigma_i^2}\right] d\alpha$$

and using the fact, taken from Eq. (A.4-14), that

$$\frac{1}{2} J_i^{o}(\rho_1+\alpha) \quad \frac{1}{2} J_i^{o}(\rho_2+\alpha) \le J_i^{o}\left(\frac{\rho_1+\rho_2}{2}+\alpha\right)$$

Consequently the minimum value of $\bar{J}_i^o(\rho)$ in Eq. (A.4-16) is achieved with the value u_i^o of u_i that minimizes $|\rho|$ subject to the constraint on the control level, as demonstrated by Fig. A.4-1. This value of u_i is easily obtained from Eqs. (A.4-3) and (A.4-15) in the following form:

$$u_{i-1}^o = \begin{cases} -\dfrac{\hat{y}_{1_{i-1}}}{\delta_{1_{i-1}}} & ; \quad \text{if} \quad \left|\dfrac{\hat{y}_{1_{i-1}}}{\delta_{1_{i-1}}}\right| \leq D \\ \pm \operatorname{sgn}\left[\dfrac{\hat{y}_{1_{i-1}}}{\delta_{1_{i-1}}}\right] ; \quad \text{if} \quad \left|\dfrac{\hat{y}_{1_{i-1}}}{\delta_{1_{i-1}}}\right| > D \end{cases} \qquad \text{(A.4-17)}$$

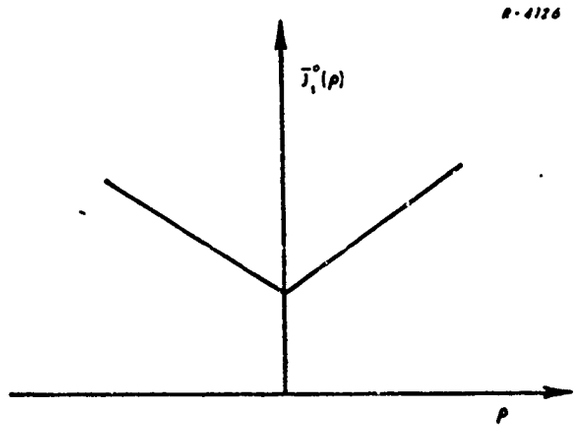

Figure A.4-1 A Graphical Illustration of the Fact that Minimizing $|\rho|$ also Minimizes any Convex Even Function of ρ.

From Eq. (A.4-17) we see that u_{i-1}^o is an <u>odd</u> function of $\hat{y}_{1_{i-1}}$; i.e.,

$$u_{i-1}^o\left(\hat{y}_{1_{i-1}}\right) = -\,u_{i-1}^o\left(-\hat{y}_{1_{i-1}}\right)$$

and therefore so is $\rho(\hat{y}_{1_{i-1}}, u_{i-1})\big|_{u_{i-1} = u^o_{i-1}}$. This implies that the optimal cost in Eq. (A.4-16), given by

$$J^o_{i-1}\left(\hat{y}_{1_{i-1}}\right) = \bar{J}^o_i(\rho)\Big|_{u_{i-1} = u^o_{i-1}}$$

is an even convex function of $\hat{y}_{1_{i-1}}$; that is, it has the same properties which we assumed for $J^o_i(\tau)$. Consequently, if $f(x_1(t_N))$ in Eq. (A.4-1) is a convex even function, so are the functions $J^o_i(\hat{y}_{1_i})$ for $i = 0, 1, \ldots, N$ and therefore Eq. (A.4-17) holds for all values of i. This result is significant for mechanizing the optimal control law because each u^o_i is given analytically in terms of the optimal estimate of the transformed state variable $\hat{y}_{1_i}$. There is no need for carrying out the integration in Eq. (A.4-13) unless the actual value of J^o_i is desired for the purpose of evaluating performance.

The above special case has been developed in detail here because it has application for tactical missile guidance systems. The discussion also demonstrates some systematic procedures -- i.e., state transformation and the use of convex, even cost functions -- that can greatly simplify the problem solution.

ANNOTATED REFERENCES

1. Stallard, D.V., "Classical and Modern Guidance of Homing Interceptor Missiles," P247, April 1968, Raytheon Company, Missile Systems Division, Bedford, Massachusetts.

This is a tutorial-type of paper describing many of the theoretical and practical aspects of homing guidance system design for tactical missiles, particularly those which use a radar seeker. A discussion of conventional proportional guidance is provided, with brief mention of optimal control and state estimation techniques. Some other topics included in the paper are: guidance accuracy, measurement noise, autopilot design, system stability, airframe design, saturation effects.

2. Stewart, E.C., "Application of Statistical Theory to Beam-Rider Guidance in the Presence of Noise," NACA RM A55E11, National Advisory Committee for Aeronautics.

The application of Wiener-filter design techniques to the problem of suppressing homing sensor measurement noise in beam-rider type guidance systems is described. Time-invariant models are used for the measurement noise statistics and performance curves are given describing miss distance as a function of noise and filter parameters.

3. Leistikow, L., et.al., "Optimum Control of Air-to-Surface Missiles," Technical Report AFFDL-TR-66-64, March 1967 (AD 815389).

The comparison in guidance accuracy achievable with pursuit, proportional, and optimal guidance laws used against surface targets is investigated. The three concepts are evaluated for a system using an inertially-aided TV homing guidance sensor. Effects of measurement noise are included. In addition, a detailed treatment of autopilot design for a missile airframe undergoing a wide change in flight conditions is presented.

4. James. J.P., "Homing Guidance," A-62-1732.3-68, Aerospace Corporation, September 14, 1962.

A simplified analytic treatment of pursuit, proportional, and biased proportional guidance concepts is presented. Each law is examined with respect to the fuel consumption it requires; the effects of accelerating targets are also investigated.

5. Garber, V., "Optimum Intercept Laws for Accelerating Targets," AIAA Journal Vol. 6, No. 11, November 1968.

Optimal Guidance Laws are derived which include the effects of time-varying target and missile accelerations in the problem formulation, and which impose an integral quadratic type penalty on control level. Analytical (algebraic) expressions for the optimal control gains as a function of time are obtained.

6. Price, C.F., "Adaptive Control and Guidance for Tactical Missiles," Vol. II, The Analytic Sciences Corporation, TR-170-1, 30 June 1970.

Performance comparisons of a wide variety of deterministic guidance laws are given, including the effects of autopilot dynamics, target acceleration, measurement bias errors and modeling errors. Performance is measured in terms of miss distance achievable versus the control effort expended.

7. Deleted [redacted]

[redacted]

8. Nahi, N.E. and Sworder, D.C., "An Optimum Interception Law with Bounded Control in Presence of Noise," AD 820631, February 1967, USCEE Report 188, Department of Electrical Engineering, University of Southern California, Los Angeles, California.

The optimum continuous-time stochastic guidance law which minimizes terminal miss distance, subject to a bounded control constraint, is derived. The mathematical model assumes that the target has constant velocity. The resulting control commands are bang-bang.

9. Sworder, D., Optimal Adaptive Control Systems, Academic Press, New York, 1966.

A textbook that treats the problem of optimal stochastic control of dicrete-time systems having unknown parameters.

10. Aoki, M., Optimization of Stochastic Systems, Academic Press, New York, 1967.

A textbook giving a general treatment of nonlinear stochastic control and estimation theory for discrete-time systems.

11. Papoulis, A., Probability, Random Variables, and Stochastic Processes, McGraw-Hill Book Co., New York, 1965.

A textbook devoted to the fundamentals of random variables and random processes.

12. Bryson, A.E., Jr., and Ho, Y.C., Applied Optimal Control, Blaisdell Publishing Co., Waltham, Massachusetts, 1969.

A textbook giving a comprehensive treatment of optimal deterministic control theory with numerous interesting examples; the theory of optimal stochastic control for linear systems with quadratic performance indices is included.

13. Jazwinski, A.H., Stochastic Processes and Filtering Theory, Academic Press, New York, 1970.

A textbook covering linear and nonlinear estimation theory from the Bayesean point of view.

14. Deyst, J.J., Jr., "Optimal Control in the Presence of Measurement Uncertainties," ScD Thesis, January 1967, Department of Aeronautics and Astronautics, The Massachusetts Institute of Technology, Cambridge, Massachusetts.

The problem of optimal stochastic control of linear systems with arbitrary performance indices is treated. A separation principle for the control law is derived which permits control commands to be computed as a function of the conditional mean of the system state. The theory is presented for both discrete and continuous time systems.

15. Dreyfus, S.E. Dynamic Programming and the Calculus of Variations, Academic Press, New York, 1965.

Methods of solving optimal control problems using both the calculus of variations and dynamic programming are presented. A particularly helpful discussion of optimal and suboptimal solutions to stochastic control problems obtained via dynamic programming is included.